Title
Short-term and long-term control of synaptic strength by light activatable glutamate receptors at the Drosophila neuromuscular junction

Author
Kauwe, Grant

Publication Date
2010

Peer reviewed|Thesis/dissertation

Short-term and long-term control of synaptic strength by light activatable glutamate receptors at the *Drosophila* neuromuscular junction

By

Grant Kauwe

A dissertation submitted in partial satisfaction of the

requirements for the degree of

Doctor of Philosophy

in

Neuroscience

in the

Graduate Division

of the

University of California, Berkeley

Committee in charge:

Professor Ehud Isacoff, chair

Professor David Bilder

Professor Mu-ming Poo

Professor Kristin Scott

Fall 2010

Short-term and long-term control of synaptic strength by light activatable glutamate receptors at the *Drosophila* neuromuscular junction

by Grant Kauwe

Abstract

Short-term and long-term control of synaptic strength by light activatable glutamate receptors at the *Drosophila* neuromuscular junction

by

Grant Kauwe

Doctor of Philosophy in Neuroscience

University of California, Berkeley

Professor Ehud Isacoff, chair

Drosophila neuromuscular junctions (NMJs) exhibit structural and physiological homeostasis during larval development in which the number of boutons and the amount of neurotransmitter released increases in coordination with larval muscle size growth. The Bone Morphogenetic Protein (BMP) signaling pathway, including Glass bottom-boat (Gbb), a BMP ligand, and Wishful thinking (Wit), its presynaptic BMP receptor, are important for regulating this homeostatic growth in larvae. Genetic analysis of Gbb suggests it is released as a retrograde signal from the postsynaptic muscle to initiate presynaptic BMP signaling for synaptic growth. However, muscle expression of Gbb fails to rescue synaptic transmission defects in the *gbb* mutant, which is instead rescued by nervous system expression of Gbb. To resolve this conflicting data and elucidate the role of Gbb at the NMJ, we investigated the expression of Gbb during *Drosophila* development at the NMJ. We fused EclipiticGFP to Gbb for visualizing its expression pattern at third-instar larval NMJs. Finally, we demonstrate genetic rescue of the *gbb* mutant with our transgenic line and provide evidence that Gbb released from the muscle may play a role in higher order synapses beyond the NMJ.

Development of the larval neuromuscular junction (NMJ) in *Drosophila* has been well characterized using genetic mutants and advanced imaging methods. However, the time course of activity-dependent changes in synaptic strength at the larval NMJ has not yet been fully investigated. To further understand the time course of synaptic plasticity at the NMJ, we used the Gal4/UAS system to express the Light-Gated Glutamate Receptor (LiGluR) in the muscle to precisely control postsynaptic activity while performing electrophysiological recordings. Our experiments reveal that long-term postsynaptic LiGluR expression during development induces a homeostatic decrease in bouton density and evoked synaptic transmission. With acute activation of LiGluRs, we potentiate synaptic transmission during high frequency stimulation. CamKII activity is required for this enhancement in synaptic strength by rapid LiGluR activation but it is not necessary for the long-term decrease in bouton density. Finally, we provide evidence that suggests the Wit BMP receptor is not required for the rapid potentiation of synaptic transmission but we provide data to possibly implicate cAMP signaling as a downstream mediator of this effect. These results suggest that a transient increase in postsynaptic

activity generated by LiGluR activation may produce a rapid retrograde signal that enhances neurotransmitter release.

Dedication

To my father, mother, and brother who have been supportive of my love for science.

Table of Contents

Acknowledgements

I would like to thank Kati Markowitz, John Ngai, and the entire Helen Wills Neuroscience Program. Thank you very much for accepting me into this prestigious program and I appreciate all your efforts in making it into what it is today. The breadth of neuroscience covered by this program is amazing and I am sure that you all will take good care of the program as it matures beyond its initial 10 years of existence. You all have been so supportive of me during my time in the program and it felt so good knowing that there are administrators that care about me.

I would like to thank John Ngai and Lu Chen for allowing me to rotate in their labs during my first year in graduate school. I appreciate the time that you spent teaching me while rotating in your labs. The research in your labs is very exciting and it was a pleasure to be a part of it for some time.

I would like to thank my professor and mentor, Ehud Isacoff. He was a wonderful mentor who always made time for me and motivated me to think broad experimentally and always "push" for the next experiment. One of my fondest memories was when I was beginning to acquire data and he asked me some questions about the electrophysiological rig setup that I did not understand, he spent the next hour at the rig going over the electrophysiological data acquisition setup with me. This was completely unplanned, yet it was so impressive how he was able to take the time out of his busy schedule to help me out. I am truly grateful to Udi's support and enthusiasm during my graduate school career and I definitely am a much more confidant and better scientist as a result of his mentorship.

I would like to thank Professors David Bilder, Mu-ming Poo, and Kristin Scott who were my graduate school thesis committee. Your scientific advice over the years was invaluable for my work. I appreciate all the time that you have taken over the years to attend my thesis committee meetings.

I would like to thank all of my labmates over the years including Sandra Wiese (who makes the lab run so smoothly), Giovanna Guerrero (who I worked with during my Iscaoff lab rotation), Robin Ball, Gautam Agarwal, Einat Peled, Steve Stowers, Francesco Tombola, Max Ulbrich, Ryan Arant, Sarah Bell, Erica Warp, Hanson Lee, Orapim Tulyathan, Medha Pathak, and the many others who helped make my time in the Isacoff lab a memorable experience. Thank you so much for all your support over the years.

I would like to thank the support of my friends over the years. I especially want to thank Dr. David Sanchez, whose support during graduate school has been indispensible for my achievement. I would like to thank all my other close friends including Todd Ferreira, Chenmei Chen, Charles Araki, 'Chelle Breeze, Osler Andres, Dane Canida, Tracey Kim, Melanie Prasol, and Dan Miranda for all their support of me during my time in graduate school. It has been great for me knowing that there are people who want me to succeed and only wish the best for my life.

I would like to thank my family, including my parents, Albert and Irene Kauwe, my brother, Blaine Kauwe, and his wife Nikki and her son Pitti, my dog Kekoa, and my aunties George, Jean, and Ellen, and my uncle Paul. Thank you so much for your support and patience during my time in graduate school. Thank you for trusting me to make these choices in life. And finally, thank you for taking the Haumana Research Program application out of the trash. If you all did not take it out of the trash, I would never have discovered my love for research.

Lastly, and certainly not least, I would like to thank Tara Tracy. Words cannot express how grateful I am for your support over the years in graduate school. Every area of my life, from research to my attitude, has been touched by your hand. Finally, to Dr. Jes Stollberg, may you rest in peace. I hope you are smiling down on me and that I have made you proud at your “old stomping ground”.

Chapter 1

Synaptic homeostasis at the *Drosophila* Neuromuscular Junction

Synaptic homeostasis: dynamic yet stable

At the most simplistic level, synapses consist of a presynaptic terminal with an active zone from which synaptic vesicles containing neurotransmitter are released. Neurotransmitter released into the synaptic cleft binds to receptors on the postsynaptic membrane thereby conveying synaptic transmission. Synaptic transmission is considered to be the primary mode of communication between a pre and post synapse, however additional trans-synaptic signaling mechanisms have been identified. Activity-dependent modifications known as synaptic plasticity can modify either pre or post synapses leading to an increase or decrease in synaptic strength. Hebbian plasticity is a synapse specific mechanism by which high frequency stimulation can strengthen synapses and low frequency stimulation can weaken synapses (Abbott and Nelson 2000; Dan and Poo 2004). How do synapses prevent runaway neuronal excitation or depression that could occur as a result of Hebbian plasticity? At the same time, how are synapses stabilized and yet remain amenable to input-dependent alterations in synaptic strength? Many studies have provided strong evidence that neurons can uniformly adjust their synaptic input by a phenomenon known as synaptic homeostasis.

Synaptic homeostasis is a mechanism by which neurons can maintain their firing rates within a dynamic range to keep network activity at a set level. One form of synaptic homeostasis is synaptic scaling where total synaptic strength is scaled up or down while preserving the relative synaptic weights and keeping the overall circuit activity at a set level. This was originally observed in mammalian cultured neurons which is where most work studying synaptic homeostasis has been performed (Turrigiano 2008).

Over a decade ago, synaptic scaling was first observed in cultured neocortical neurons. This original study illustrates many of the common techniques used to investigate synaptic homeostasis. They showed that chronic activity blockade of cultured cortical neurons with tetrodotoxin (TTX), a blocker of voltage gated Na+ channels, increased the amplitude of miniature excitatory postsynaptic currents (mEPSCs). This suggests that neurons increase either the number and/or activity of postsynaptic AMPA-type glutamate receptors to compensate for the global reduction in circuit activity. To investigate the physiological response to a prolonged increase in network activity, they blocked $GABA_A$ receptor activity with a chronic treatment of bicuculline. With this treatment they observed a scaled decrease in mEPSC amplitudes signifying an overall reduction in excitatory synaptic input while neuronal firing rates were maintained close to untreated control levels. For manipulations involving the increase or decrease in network activity, cultures were treated with their respective pharmacological drugs for 48 hours. Importantly, they found that the amplitude of mEPSCs scaled by a multiplicative factor thereby keeping the relative synaptic strengths intact (Turrigiano, Leslie et al. 1998).

These experiments demonstrate the primary mechanism of synaptic homeostasis allowing neurons to appropriately compensate for chronic changes in activity by altering the level of presynaptic function and/or postsynaptic response in order to maintain a standard level of network activity (Figure 1.1). In research on homeostatic synaptic

plasticity, a commonly used approach to assess uniform changes in synaptic function is to record postsynaptic miniature spontaneous activity after chronic pharmacological treatment. Prolonged changes in network activity induced by drug treatment often leads to a robust homeostatic effect observed in neurons. Furthermore recordings of mEPSCs are a relatively straightforward electrophysiological readout that reveals the direction of the homeostatic response (ie. synapse strengthening or weakening) and the potential mechanism underlying the expression of this plasticity. An increase or decrease in the frequency of miniature spontaneous release suggests a change in synaptic vesicle release probability or in the number of functional synapses (Bacci, Coco et al. 2001; Burrone, O'Byrne et al. 2002). A change in the amplitude of miniature spontaneous events usually corresponds to a change in the number or postsynaptic receptors or in the receptor channel properties (O'Brien, Kamboj et al. 1998; Turrigiano, Leslie et al. 1998). Despite these advantages, studies using cultured neurons lack the specific anatomical structures and cellular architecture found *in vivo* that could influence homeostatic synaptic plasticity in response to changes in network activity (Pozo and Goda 2010). As a complement to neuronal culture experiments, the *Drosophila* neuromuscular junction provides a platform on which mechanisms underlying synaptic homeostasis can be investigated in a simplified, highly patterned environment that takes advantage of all the genetic tools and techniques associated with the *Drosophila* model system.

The *Drosophila* neuromuscular junction

The *Drosophila* larval neuromuscular junction (NMJ) is a glutamatergic synapse that exhibits functional properties and molecular components that are very similar to excitatory synapses in the mammalian central nervous system. There are several types of plasticity expressed at the NMJ, including short-term synaptic plasticity and synaptic homeostasis. The fly NMJ is amenable to a variety of experimental approaches, including electrophysiological, imaging, and genetic techniques, making it a powerful model system to examine synapse function (Ruiz-Canada and Budnik 2006).

Glutamatergic synaptic transmission at the *Drosophila* NMJ can be easily evaluated by using electrophysiological techniques. The most commonly used preparation for electrophysiological recordings requires the dissection of third-instar larvae into a fillet which provides internal access to NMJs. The larval muscles are easily identifiable due to their large size and highly stereotyped body wall structure (Budnik, Gorczyca et al. 2006) (Figure 1.2). To assess synaptic activity at the larval NMJ, we can do single electrode recordings under current clamp mode to monitor either miniature excitatory junctional potentials (mEJPs), representing the spontaneous release of glutamate-containing vesicles, or excitatory junctional potentials (EJPs), which are responses evoked by nerve stimulation (Figure 1.3A). In addition to this, we can perform two-electrode voltage clamp of the muscle and record miniature excitatory junctional currents (mEJCs) and evoked excitatory junctional currents (EJCs) (Imlach and McCabe 2009; Zhang and Stewart 2010) (Figure 1.3B). For most experiments, we used the two electrode voltage clamp technique to acquire an accurate readout of synaptic transmission through glutamate receptors without contribution from voltage-gated ion channels. Recordings in voltage clamp mode are also used to prevent

nonlinear summation of synaptic activity during high frequency stimulation. Voltage clamping the muscle requires the use of two intracellular electrodes, one for recording voltage and another for injecting current. A third electrode is used to suck up the free nerve ending of the NMJ for electrical stimulation to induce action potentials (Figure 1.4). For monitoring spontaneous miniature synaptic transmission, we used current clamp mode because of the improved signal-to-noise ratio in recordings (Figure 1.4 inset).

In combination with electrophysiology, we can perform live imaging of synaptic activity at the NMJ. Glutamate receptors at the NMJ are calcium permeable, making it possible to monitor synaptic activity using fluorescent calcium dyes or genetically encoded fluorescent protein calcium indicators. For decades, calcium indicators have been used to examine synaptic transmission, however, disadvantages in using these dyes include difficulty in loading into tissues, lack of cell specificity, and inability to target dyes at sub-cellular sites (Griesbeck 2004). To specifically image presynaptic activity at the NMJ, calcium dyes have to be loaded for 20-40 minutes into cut motor axons (Macleod, Hegstrom-Wojtowicz et al. 2002). On the other hand, genetically encoded calcium indicators can be expressed in specific tissue and targeted to sub-cellular sites (Chudakov, Lukyanov et al. 2005). For example, our laboratory has accomplished single bouton resolution calcium imaging with the development of a genetically encoded calcium indicator (GECI) fused to a CD8 membrane domain and the Shaker C terminus. This chimeric calcium sensor is targeted specifically to the intracellular plasma membrane at postsynaptic sites (Guerrero, Reiff et al. 2005). While electrophysiological recordings of EJCs represents the summed postsynaptic activity across all boutons, single bouton calcium imaging improves the spatial resolution for monitoring synaptic activity at the NMJ, thereby giving us more information on synapse specific changes in synaptic transmission.

The hallmark of *Drosophila* research is the variety of genetic tools that are available. The Gal4 yeast transcription factor and its target upstream activation sequence (UAS) constitutes the most commonly used expression system in *Drosophila*. The beauty of the Gal4/UAS system is that flies expressing a UAS transgene can be crossed with any Gal4 expressing fly line to transcribe UAS target genes with high temporal and spatial precision (Brand and Perrimon 1993). At the NMJ, the Gal4/UAS system can express genes at either the pre- or postsynaptic side for studying molecular mechanisms involved in synaptic function. To extend the temporal resolution of Gal4/UAS, the temperature sensitive Gal80ts can be used to repress Gal4 during development at the permissive temperature. Conversely Gal80ts can be inactivated at the restrictive temperature to allow for Gal4 transcription (Figure 1.5) (McGuire, Le et al. 2003). Using this expression system alongside the plethora of genetic mutants and tools for monitoring activity provides a strong basis for studies of synaptic function at the NMJ.

Synaptic homeostasis at the *Drosophila* neuromuscular junction

Through genetic manipulations during development previous work has demonstrated the importance of long-term retrograde signaling in synaptic homeostasis. It was observed in the *gluRIIA* mutant that a retrograde signal from the muscle instructs the presynaptic neuron to compensate for reduced activity by increasing quantal content. This suggests that reduced receptor activity during muscle growth is compensated by increased presynaptic function to promote efficient postsynaptic depolarization. Despite this compensation, the *gluRIIA* mutant NMJs exhibit normal bouton and active zone numbers which could indicate that the dependence of morphological development on physiological synaptic homeostasis (Petersen, Fetter et al. 1997). The *gluRIIA* mutant exemplifies a well-characterized model of synaptic homoestasis at the NMJ.

Interestingly, postsynaptic overexpression of GluRIIA increases mEJP and evoked EJP amplitudes but does not result in a compensatory decrease in quantal content. It is possible that postsynaptic muscle activity may never exceed presynaptic input during development (Petersen, Fetter et al. 1997). Similarly, postsynaptic inhibition of PKA activity results in an increase in mEJC and evoked EJC amplitudes but no compensatory decrease in quantal content (Davis, DiAntonio et al. 1998). These two different methods to increase postsynaptic quantal size fail to induce a compensatory decrease in quantal content.

In addition to these previous results, it has been show that an increase in muscle innervation by postsynaptic overexpression of FasII results in a decrease in vesicle release probability at single boutons as assessed by extracellular recordings from individual boutons. These hyperinnervated muscles exhibit only a modest decrease in quantal content, which is far less than expected despite the significant increase in bouton growth (Davis and Goodman 1998). Indeed, a discrepancy exists where a postsynaptic increase in quantal size does not induce a compensatory decrease in presynaptic function yet an increase in muscle innervation results in a decrease in presynaptic release probability. One possible explanation is that the muscle monitors some signal from increased muscle innervation to reduce vesicle release probability that is independent of GluRIIA activation. This signal could come in the form of glutamate release detected by an unknown postsynaptic glutamate receptor or the release of an unidentified signal by presynaptic boutons. Alternatively, the presynapse could self-regulate its vesicle release probability based on the density of boutons (Davis and Goodman 1998). It remains to be determined whether or not there are alternative manipulations of increasing postsynaptic activity that could uncover synaptic homeostatic mechanisms to decrease presynaptic strength.

In addition to the importance of long-term retrograde signaling on synapse development at the NMJ, rapid induction of retrograde signaling for maintaining synaptic function has been uncovered at the *Drosophila* NMJ. Similar to presynaptic homeostatic compensation in *gluRIIA* mutants, a rapid increase in quantal content can be observed within minutes through pharmacological inhibition of postsynaptic glutamate receptors

(Frank, Kennedy et al. 2006). Recent evidence suggests that the BMP signaling pathway acts as the retrograde signal to induce the rapid presynaptic increase in quantal content (Goold and Davis 2007). Interestingly, a mutation for *ephexin*, a guanine nucleotide exchange factor, is necessary for the induction of sustained synaptic homeostasis in the *glurIIA* mutant and yet is not required for rapid synaptic homeostasis induced by pharmacology (Frank, Pielage et al. 2009). The observation that synaptic homeostasis can occur within minutes raises the possibility the other types of retrograde signaling could be triggered rapidly at the NMJ.

Another example of rapid retrograde signaling at the NMJ has been shown in *syt 4* mutant. Syt 4 is a postsynaptically localized isoform of synaptotagmin found at the NMJ. Directly following a high frequency stimulation of the NMJ for 1 minute there is an increase in spontaneous vesicle release that is observed. In *syt 4* mutants, this stimulus induced increased frequency of miniature responses is impaired however it is rescued by postsynaptic expression of Syt 4. It appears that this form of synaptic plasticity requires presynaptic cAMP-PKA signaling. Expression of the temperature-sensitive *shibire*, the *Drosophila* dynamin protein required for endocytosis, in the muscle at the restrictive temperature can also disrupt this retrograde signal required for induction of high frequency miniature release. These results suggest the presence of postsynaptic vesicle release machinery that may be important for rapidly modulating presynaptic function (Yoshihara, Adolfsen et al. 2005).

Thesis summary

Here, we provide evidence that the putative retrograde BMP ligand, Glass bottom boat (Gbb), is released from the postsynaptic muscle and trafficked back to the motor neuron cell body and beyond to higher order synapses. This would suggest that Gbb is important as a retrograde signal for coordinating synaptic strength in the larval motor circuit. In addition to this, we have found a significant decrease in bouton density and evoked synaptic transmission as a result of long-term postsynaptic expression of Light Activatable Glutamate Receptors at NMJs. This provides evidence for a mechanism at NMJs whereby increases in postsynaptic activity can be compensated by a decrease in presynaptic function. Finally, we report evidence for what might be a rapid retrograde signaling pathway that potentiates synaptic function. Initial experiments suggest that this signaling is independent of the BMP pathway and instead entails postsynaptic CAMKII activation and may require cAMP activity. Here we demonstrate the versatility of the Light Activatable Glutamate Receptors as a tool to investigate two different phenomena involving long-term or short-term changes in synaptic activity.

Figure 1.1

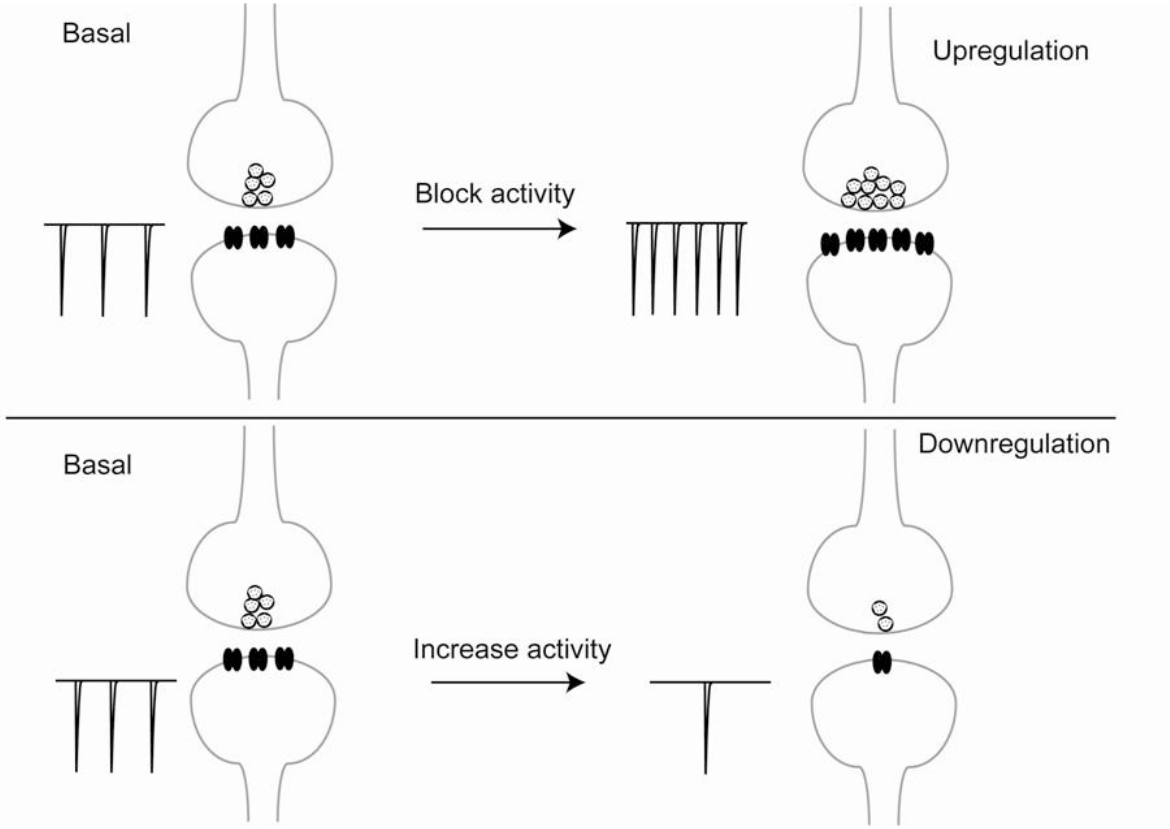

Figure 1.1. Chronic changes in network activity induce synaptic homeostasis.

Cartoon depicts synaptic homeostasis in neurons where a chronic pharmacological blockade of activity could result in an increase in the number and/or function of postsynaptic receptors or an increase in presynaptic vesicle release (top). Chronically increasing activity could result in a decrease in number and/or function of postsynaptic receptors or a decrease in presynaptic vesicle release (bottom).

Figure 1.2

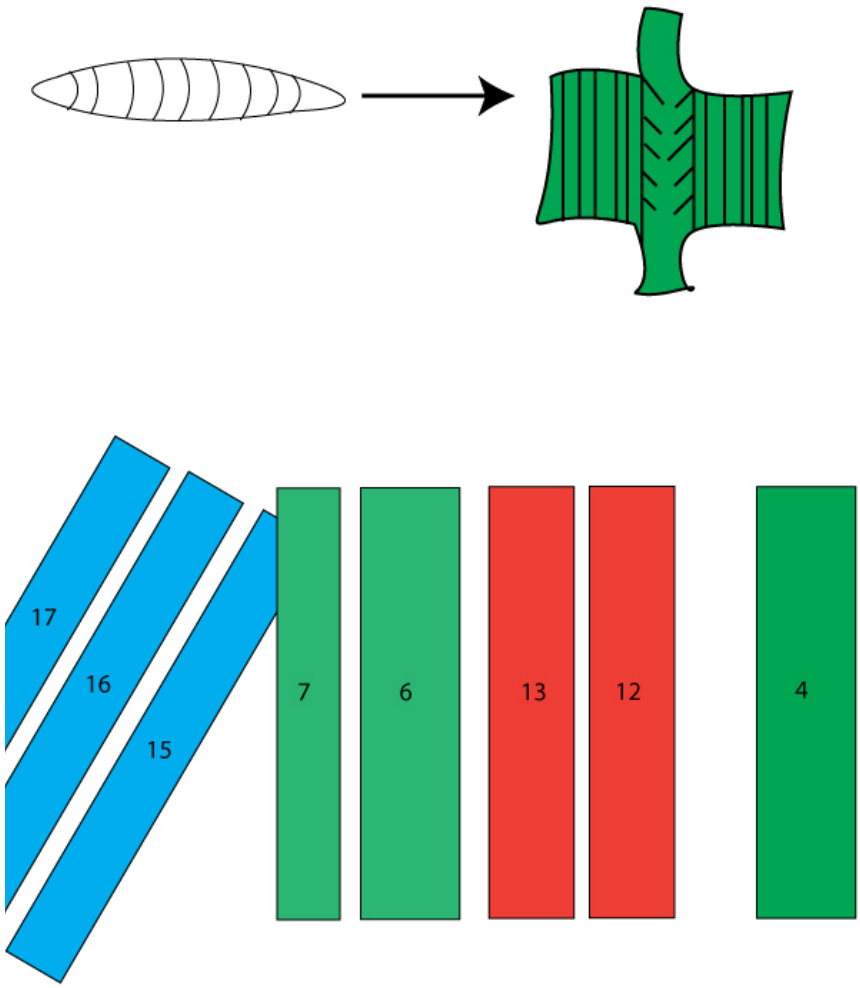

Figure 1.2. Larval muscles exhibit a stereotyped structure.

Cartoon depicts a larva which is dissected into a fillet form to allow access for electrophysiology and imaging experiments to study NMJ function (top). NMJs exhibit a patterned structure that allows for easy identification of muscles for experiments. NMJs on muscle 6 and muscle 4 are commonly used in experiments because of their relatively large size (bottom).

Figure 1.3

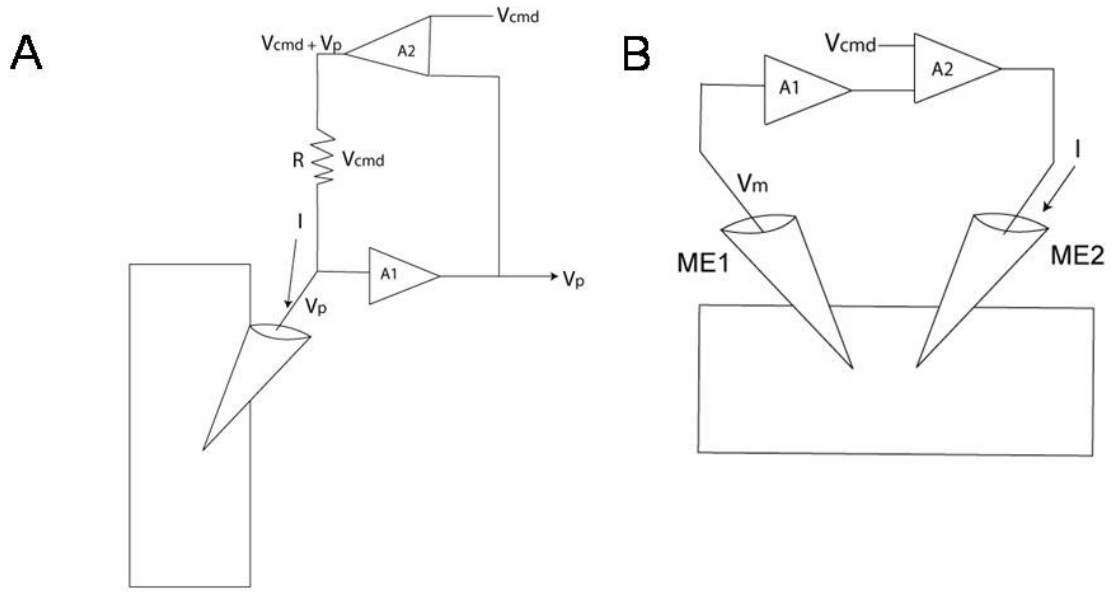

Figure 1.3. Schematic of single electrode current clamp and two-electrode voltage clamp recordings.

(A) Current clamp recordings can be performed with a single electrode where an amplifier (A1) can monitor voltage at the electrode tip (V_p). A second amplifier (A2) can be added to the circuit that can inject current into the cell such that $I = V_{cmd}/R$. The voltage across the resistor (R) is equal to V_{cmd} regardless of V_p**. (B)** Two electrode voltage clamp recordings can be performed where the ME1 electrode records voltage in the cell (V_m) through an amplifier (A1). V_m is compard to V_{cmd} in a second amplifier (A2) where the output of A2 depends on the difference between V_m and V_{cmd}. Current output of A2 flows through ME2 electrode into the cell.

Figure 1.4

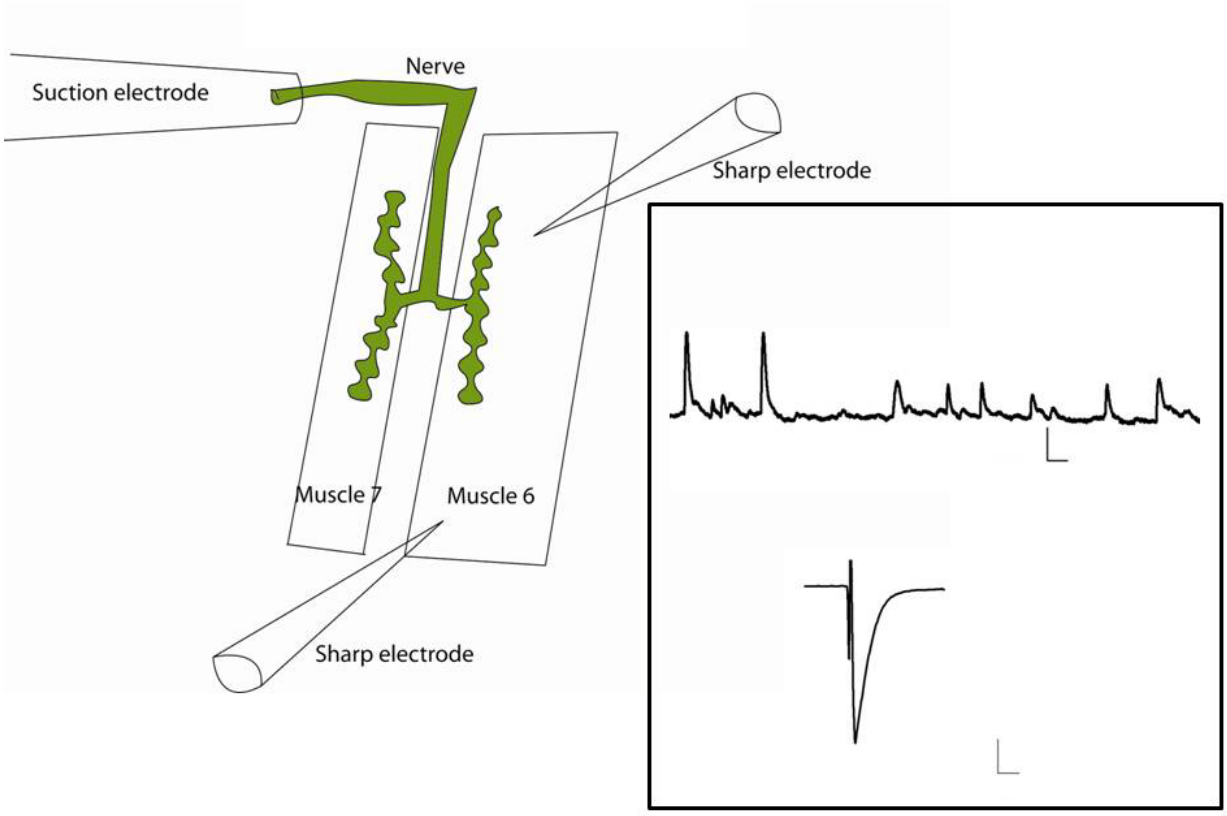

Figure 1.4. Diagram of electrophysiological recordings at the NMJ and example traces.

Cartoon depicts electrophysiology setup at for two electrode voltage clamp recordings at muscle 6 NMJs. One intracellular electrode is for recording voltage and a second is for injecting current. A third suction electrode is used to suck up a free nerve for electrical stimulation to induce action potentials which evoke neurotransmitter release at NMJs. Both intracellular electrodes are placed near the center of muscle 6 but positioned away from boutons near the midline of muscle 6/7 NMJs. Example traces of mEJPs (top inset) and evoked EJCs (bottom inset) are displayed. Scale bar for mEJP trace is 1 mV and 100 ms. Scale bar for evoked EJC is 50 nA and 10 ms.

Figure 1.5

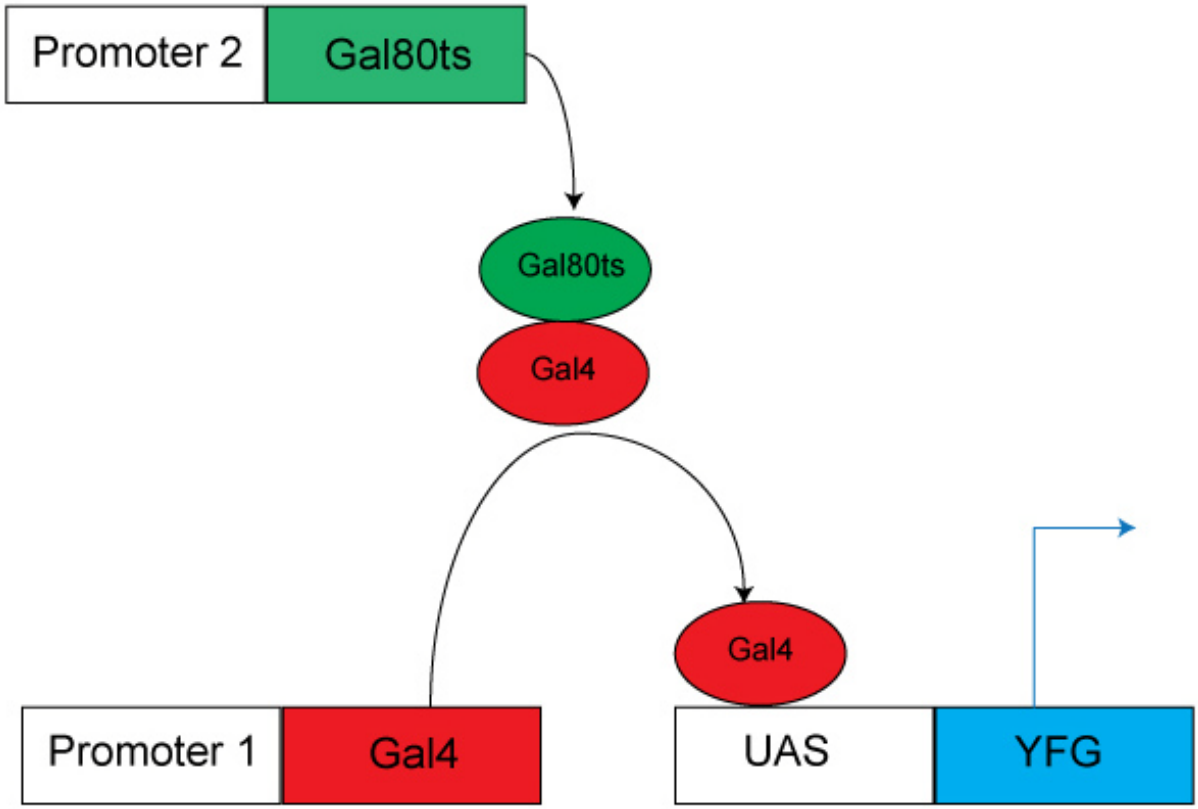

Figure 1.5. Schematic of Gal4/UAS expression system with Gal80 inhibition.

The transcription of Gal4 protein is under the control of an enhancer/promoter for temporal and spatial specificity of expression. Gal4 protein binds to the upstream activation sequence (UAS) sequence to initiate transcription of your favorite gene (YFG). To increase temporal control of Gal4/UAS expression, temperature sensitive Gal80ts can be expressed in the same fly, usually under the control of a ubiquitous promoter (ie. tubulin promoter). At the permissive temperature of 18°C, Gal80ts is active and binds to the transcription activation domain of Gal4 to prevent Gal4 mediated expression (depicted in cartoon). At the restrictive temperature of 30°C, Gal80ts protein is inactivated, thus allowing Gal4 to induce transcription of YFG.

References

Abbott, L. F. and S. B. Nelson (2000). "Synaptic plasticity: taming the beast." Nat Neurosci **3 Suppl**: 1178-1183.

Bacci, A., S. Coco, et al. (2001). "Chronic blockade of glutamate receptors enhances presynaptic release and downregulates the interaction between synaptophysin-synaptobrevin-vesicle-associated membrane protein 2." J Neurosci **21**(17): 6588-6596.

Brand, A. H. and N. Perrimon (1993). "Targeted gene expression as a means of altering cell fates and generating dominant phenotypes." Development **118**(2): 401-415.

Budnik, V., M. Gorczyca, et al. (2006). "Selected methods for the anatomical study of Drosophila embryonic and larval neuromuscular junctions." Int Rev Neurobiol **75**: 323-365.

Burrone, J., M. O'Byrne, et al. (2002). "Multiple forms of synaptic plasticity triggered by selective suppression of activity in individual neurons." Nature **420**(6914): 414-418.

Chudakov, D. M., S. Lukyanov, et al. (2005). "Fluorescent proteins as a toolkit for in vivo imaging." Trends Biotechnol **23**(12): 605-613.

Dan, Y. and M. M. Poo (2004). "Spike timing-dependent plasticity of neural circuits." Neuron **44**(1): 23-30.

Davis, G. W., A. DiAntonio, et al. (1998). "Postsynaptic PKA controls quantal size and reveals a retrograde signal that regulates presynaptic transmitter release in Drosophila." Neuron **20**(2): 305-315.

Davis, G. W. and C. S. Goodman (1998). "Genetic analysis of synaptic development and plasticity: homeostatic regulation of synaptic efficacy." Curr Opin Neurobiol **8**(1): 149-156.

Davis, G. W. and C. S. Goodman (1998). "Synapse-specific control of synaptic efficacy at the terminals of a single neuron." Nature **392**(6671): 82-86.

Frank, C. A., M. J. Kennedy, et al. (2006). "Mechanisms underlying the rapid induction and sustained expression of synaptic homeostasis." Neuron **52**(4): 663-677.

Frank, C. A., J. Pielage, et al. (2009). "A presynaptic homeostatic signaling system composed of the Eph receptor, ephexin, Cdc42, and CaV2.1 calcium channels." Neuron **61**(4): 556-569.

Goold, C. P. and G. W. Davis (2007). "The BMP ligand Gbb gates the expression of synaptic homeostasis independent of synaptic growth control." Neuron **56**(1): 109-123.

Griesbeck, O. (2004). "Fluorescent proteins as sensors for cellular functions." Curr Opin Neurobiol **14**(5): 636-641.

Guerrero, G., D. F. Reiff, et al. (2005). "Heterogeneity in synaptic transmission along a Drosophila larval motor axon." Nat Neurosci **8**(9): 1188-1196.

Imlach, W. and B. D. McCabe (2009). "Electrophysiological methods for recording synaptic potentials from the NMJ of Drosophila larvae." J Vis Exp(24).

Macleod, G. T., M. Hegstrom-Wojtowicz, et al. (2002). "Fast calcium signals in Drosophila motor neuron terminals." J Neurophysiol **88**(5): 2659-2663.

McGuire, S. E., P. T. Le, et al. (2003). "Spatiotemporal rescue of memory dysfunction in Drosophila." Science **302**(5651): 1765-1768.

O'Brien, R. J., S. Kamboj, et al. (1998). "Activity-dependent modulation of synaptic AMPA receptor accumulation." Neuron **21**(5): 1067-1078.

Petersen, S. A., R. D. Fetter, et al. (1997). "Genetic analysis of glutamate receptors in Drosophila reveals a retrograde signal regulating presynaptic transmitter release." Neuron **19**(6): 1237-1248.

Pozo, K. and Y. Goda (2010). "Unraveling mechanisms of homeostatic synaptic plasticity." Neuron **66**(3): 337-351.

Ruiz-Canada, C. and V. Budnik (2006). "Introduction on the use of the Drosophila embryonic/larval neuromuscular junction as a model system to study synapse development and function, and a brief summary of pathfinding and target recognition." Int Rev Neurobiol **75**: 1-31.

Turrigiano, G. G. (2008). "The self-tuning neuron: synaptic scaling of excitatory synapses." Cell **135**(3): 422-435.

Turrigiano, G. G., K. R. Leslie, et al. (1998). "Activity-dependent scaling of quantal amplitude in neocortical neurons." Nature **391**(6670): 892-896.

Yoshihara, M., B. Adolfsen, et al. (2005). "Retrograde signaling by Syt 4 induces presynaptic release and synapse-specific growth." Science **310**(5749): 858-863.

Zhang, B. and B. Stewart (2010). "Voltage-clamp analysis of synaptic transmission at the Drosophila larval neuromuscular junction." Cold Spring Harb Protoc **2010**(9): pdb prot5488.

Chapter 2

Fluorescently tagged Glass Bottom Boat reveals the expression pattern of a retrograde signal

Introduction

The Bone Morphogenetic Protein (BMP) signaling pathway has been shown to be required for the proper development of the *Drosophila* NMJ (Aberle, Haghighi et al. 2002; Marques, Bao et al. 2002). The current model for BMP signaling at the NMJ involves the release of the putative ligand, Glass Bottom Boat (Gbb), from the postsynaptic muscle initiating a retrograde signal by binding to the presynaptic heterodimer receptor composed of the Type II BMP receptor Wishful Thinking (Wit) and either Type I receptor partner Saxophone (Sax) or Thickveins (Tkv). The activation of this receptor complex leads to receptor mediated phosphorylation of the Smad protein, Mothers Against Decapentaplegic (Mad). The phosphorylation of Mad is thought to occur at nerve terminals which results in the retrograde transport of pMad back to the motor neuron cell body to act as a transcription factor that regulates synaptic growth (McCabe, Marques et al. 2003). A recent study suggest that transcription of Rac guanine exchange factor Trio is in fact regulated by pMad and is necessary for proper synaptic growth through BMP signaling at the NMJ (Ball, Warren-Paquin et al. 2010).

Despite past efforts to delineate the proteins involved in the BMP signaling pathway at the NMJ, we still do not have a clear understanding of how Gbb is released during synapse development. The expression pattern of Gbb has not been characterized at the NMJ, and moreover, the time course of its retrograde signaling during development remains unclear. To investigate the regulation of Gbb signaling at the NMJ, we decided to generate transgenic flies expressing a fluorescently tagged Gbb. In order to do this, we created UAS transgenic lines containing Gbb fused to fluorescent reporters which we could use in the Gal4/UAS expression system to drive expression of Gbb fusion constructs in the muscle. We chose to make one transgenic Gbb fluorescent protein fusion line expressing monomeric red fluorescent protein (mRFP) as a constitutively active fluorescent reporter of Gbb localization (Campbell, Tour et al. 2002). We decided to construct another transgenic Gbb fluorescent protein fusion line with the ph-sensitive superecliptic GFP (Miesenbock, De Angelis et al. 1998). We hypothesized that if Gbb is contained in acidified postsynaptic vesicles, then superecliptic GFP fluorescence would be quenched. Upon vesicular release of Gbb, the superecliptic GFP conjugated Gbb would fluoresce as it enters the more basic extracellular environment, thus allowing us to monitor its release with temporal specificity.

Results and Discussion

Creation of Gbb fluorescent protein fusion constructs

The Gbb cDNA sequence is 1667 base pairs long and consists of a 1365 base pair protein coding region. The Gbb protein consists of an N-terminus signal sequence which is followed by a propeptide region and the C-terminus mature ligand region. There are multiple proteolytic cleavage sites that exist between the propeptide region and ligand. The Gbb ligand cannot function properly without first being cleaved from the propeptide region (correspondence with Dr. Brian Mccabe). Furthermore, the C-terminus of Gbb plays a role in dimerization of the ligand (Wharton, Thomsen et al. 1991). To determine the best site of fusion for a fluorescent tag on Gbb, we had to take all of these factors into consideration.

To help with our cloning strategy, we turned to previous work done with another BMP ligand in Drosophila, Decapentaplegic (Dpp). Two papers had published work showing expression of Dpp during fly development using GFP fusions to Dpp. Enchev et al. inserted GFP at an internal location that was 9 amino acids into the mature ligand domain, thus avoiding any potential cleavage sites or impacting N or C-terminus domains of Dpp (Entchev, Schwabedissen et al. 2000). Teleman et al. inserted GFP downstream of the proteolytic cleavage sites and at the N-terminus of the mature ligand domain of Dpp (Teleman and Cohen 2000). With two successful approaches used to fuse fluorescent proteins to Dpp, we decided to take the former approach and clone our fluorescent protein fusions internally into the mature ligand domain.

We cloned mRFP and superecliptic GFP at a location that was 12 amino acids downstream of the N-terminus portion of the Gbb mature ligand (Figure 2.1). Both constructs were separately cloned into the pUAST vector to be made into transgenic fly lines. Importantly, the mature ligand of Gbb is about 100 amino acids, whereas GFP is 238 amino acids. This underscores how much larger the tagged ligand is made by the addition of GFP, thus the fluorescent protein fusions to Gbb could be expected to inhibit the functionality of the Gbb protein.

When we expressed our UAS transgenic lines with 24B-Gal4 driver we observed very strong expression in the muscles as expected. We noticed that a specific column of cells on the dorsal midline appeared to fluoresce much brighter in the mRFP-Gbb line as compared to the superecliptic GFP-Gbb line. This could be due to the pH sensitive nature of the superecliptic GFP-Gbb which we expected to be quenched in acidic vesicles (Figure 2.2A,B left panels). When we looked at muscle expression between both transgenic lines in dissected larval fillets, we did not observe any salient differences between either line. (Figure 2.2A,B right panels). We decided to further characterize Gbb expression using the superecliptic GFP-Gbb line.

We were next interested in observing superecliptic GFP-Gbb expression at NMJs. We fixed and stained larval NMJs expressing superecliptic GFP-Gbb in muscles with antibodies to GFP and HRP (neuronal marker). We detected GFP throughout the muscle from postsynaptic expression of superecliptic GFP-Gbb (Figure 2.3). Interestingly, we observed GFP antibody labeling in the motor neuron axon despite using a Gal4 driver that specifically expresses in muscles (Figure 2.3B white arrow).

This suggests that superecliptic GFP-Gbb is trafficked beyond nerve terminals to the motor neuron cell body.

Postsynaptic expression of UAS-superecliptic GFP-Gbb rescues *gbb* mutant synaptic growth

Since we successfully detected expression of our fluorescent protein fusions to Gbb in our transgenic lines, we next tested for rescue of the *gbb* mutant phenotype to show that these fusion proteins expressed in larvae can recapitulate native Gbb function. Previous work has shown that postsynaptic muscle expression of Gbb in the *gbb* mutant background completely rescues bouton growth while only partially rescuing synaptic physiology. Neuronal expression of Gbb completely rescues synaptic physiology deficits in the *gbb* mutant but does not rescue the synaptic growth deficit phenotype.

To test for rescue of the *gbb* mutant with our transgenic Gbb lines, we used the G14-Gal4 muscle driver, the same driver used in the original Gbb rescue experiments, to drive UAS-superecliptic GFP-Gbb expression in muscles (McCabe, Marques et al. 2003). We calculated bouton density and observed a significant decrease in *gbb* mutant NMJs as compared to wild-type NMJs. When we examined bouton density in NMJs expressing UAS-superecliptic GFP-Gbb with G14-Gal4 in *gbb* mutants, we observed no significant difference in bouton density as compared to wild-type NMJs ($p = 0.860$) (Figure 2.4A-E). We next recorded evoked excitatory junctional currents (EJCs) from NMJs and observed a significant decrease in the amplitude of evoked EJCs in *gbb* mutants. However, when we recorded from NMJs expressing UAS-superecliptic GFP-Gbb with G14-Gal4 in the *gbb* mutant background, we observed an expected partial rescue of evoked EJC amplitudes (Figure 2.4F). Our rescue data for synaptic physiology and bouton density with superecliptic GFP-Gbb is consistent with previously published results and suggests that our construct recapitulates the function of native Gbb.

However, it is possible that in our transgenic flies the superecliptic GFP protein could be cleaved from Gbb before it is released from the muscle. To determine whether or not this occurs, we could use western blot analysis of lysates from flies expressing either superecliptic GFP-Gbb or native Gbb. We would expect to observe a shift in the size of Gbb to a higher molecular weight with the fluorescent tag unless superecliptic GFP is in fact removed by proteolytic cleavage in the muscle. This experiment would require having access to a working antibody against Gbb or expressing another epitope tagged version of Gbb.

Postsynaptic muscle expression of Gbb is trafficked to the motor neuron cell body

With evidence that our transgenic superecliptic GFP-Gbb line rescues the *gbb* mutant phenotype, we returned to analyzing its expression in the nervous system. We previously observed that when we use an antibody to GFP at NMJs expressing superecliptic GFP-Gbb in the muscle, we detect expression in motor neuron axons. We

next wanted to take a closer look at how postsynaptic muscle expression of superecliptic GFP-Gbb appears in the ventral nerve cord where motor neuron cell bodies are located. We dissected third-instar larvae while keeping the brain intact and did live imaging of superecliptic GFP-Gbb in the larval central nervous system. Surprisingly, we observed fluorescence in what appears to be motor neuron cell bodies in the ventral nerve cord and in neurons located in either hemisphere of the optic lobes despite our selective expression of superecliptic GFP-Gbb in the muscles (Figure 2.5). Indeed, the role of Gbb derived from the muscle was thought to be limited to synaptic function at NMJs but here we provide evidence that muscle derived Gbb may in fact be important at higher-order synapses.

Our initial discovery of superecliptic GFP-Gbb expression in the optic lobe was done using epifluorescent imaging, so we next decided to acquire confocal resolution images of this expression in the optic lobe. As a control for our superecliptic GFP-Gbb imaging, we expressed GFP in the muscle with the same Gal4 driver in separate larvae to examine the possibility that high levels of GFP expression in the muscle could also be trafficked into the nervous system. For these experiments, we used an antibody to GFP and exposed both control and superecliptic GFP-Gbb expressing NMJs to the same treatment. When we imaged the optic lobe expressing superecliptic GFP-Gbb in the muscle, we detected expression in a subset of neurons in the optic lobe. We did not detect significant expression of GFP in the control optic lobe (Figure 2.6). This provides strong evidence for the retrograde trafficking of superecliptic GFP-Gbb into the motor axon, back to the cell body, and beyond to higher order synapses.

It would be important in the future to repeat these imaging experiments in the optic lobe and ventral nerve cord to quantify the localization of superecliptic GFP-Gbb in the ventral nerve cord and optic lobe across multiple larval preparations and experiments. This would be very important to verify our initial findings with statistical significance before continuing further experiments.

Interestingly at the 2009 Cold Spring Harbor Neurobiology of Drosophila meeting, a talk given by professor Guillermo Marques showed that the receptor for Gbb, Wishful Thinking and a type I BMP receptor, forms a complex that is trafficked back from the nerve terminal to the motor neuron cell body. He displayed movies of fluorescently tagged versions of these BMP receptors moving in the retrograde direction in the motor neuron axons. Finally, he showed that in *gbb* mutants, this complex did not move in the retrograde direction which suggests that Gbb bound to the BMP receptor heterodimer complex is required for retrograde transport of the BMP signal to the motor neuron cell body for phosphorylation of Mad. Our data from the superecliptic GFP-Gbb experiments support this hypothesis such that we observed superecliptic GFP-Gbb expression in the motor neuron cell bodies when we expressed it only in postsynaptic muscles providing evidence that Gbb is indeed trafficked in a retrograde manner back to the motor neuron cell body.

Future experiments

In the future, we would repeat the experiments using superecliptic GFP-Gbb in the *wit* or *gbb* mutant background. In the *wit* mutant background, one would not expect to observe superecliptic GFP-Gbb expression in the ventral cord if it is expressed with a Gal4 muscle driver if Gbb binding to the Wit receptor is required for retrograde trafficking. This experiment would conclude that the observed expression of fluorescently tagged Gbb in the motor neuron requires the presence of the Wishful Thinking BMP receptor and it would provide additional evidence that the fluorescently tagged Gbb faithfully reproduces the activity of the native Gbb ligand. In addition, it would be important to use superecliptic GFP-Gbb in the *gbb* mutant background to prevent the contribution of endogenous Gbb from outcompeting and reducing its effectiveness, and by doing experiments in the *gbb* mutant, we could argue that our results are derived from our transgenic Gbb and not endogenous Gbb.

Another intriguing question about the expression of superecliptic GFP-Gbb is the possibility that it is being trafficked across multiple synapses. We previously observed that muscle expression of superecliptic GFP-Gbb results in fluorescence detected in the optic lobes of third-instar larvae. It is conceivable to think that the superecliptic GFP-Gbb must transverse through multiple synapses to reach the optic lobe since the only source of superecliptic GFP-Gbb is from the muscle. To further examine the expression pattern of Gbb, we could construct another fluorescently tagged Gbb using photoactivatable GFP. Using this approach, we could selectively photoactivate GFP-Gbb in the muscles and monitor its expression pattern during development (Patterson and Lippincott-Schwartz 2002). This experiment would be useful to investigate the time course of the retrograde transport of Gbb following GFP photoactivation in the muscle. Previous work has shown that BMP signaling, including Gbb, is required for synaptic strengthening between presynaptic cholinergic neurons and postsynaptic motorneurons in the larval ventral nerve cord (Baines 2004). Indeed, BMP signaling appears to be important for synapse development at both the NMJ and synapses in the larval CNS. Our surprising finding that superecliptic GFP-Gbb was transported all the way from the muscles to synapses of the CNS raises the question: What functional role might Gbb released from the muscle play at synapses onto the motoneurons? We could take an electrophysiologcal approach with the *gbb* mutant to determine whether or not superecliptic GFP-Gbb expressed in the muscle can rescue synaptic strengthening at cholinergic motorneuron synapses in the larval ventral nerve cord. We could then have functional evidence that suggests Gbb from the postsynaptic muscle is required for the development of motorneuron synapses in the larval CNS. To further understand the expression pattern of Gbb, we could monitor the expression of superecliptic GFP-Gbb in mutants that alter the level of BMP signaling, such as the *nervous wreck* mutant, where BMP signaling occurs unrepressed which results in synaptic overgrowth, and monitor how the time course and amount of Gbb signaling is altered (O'Connor-Giles, Ho et al. 2008). We hypothesize that Gbb could be acting across multiple synapses as a signal to coordinate the larval motor circuit from brain to muscle so that all synapses within the circuit are strengthened cooperatively.

Figure 2.1

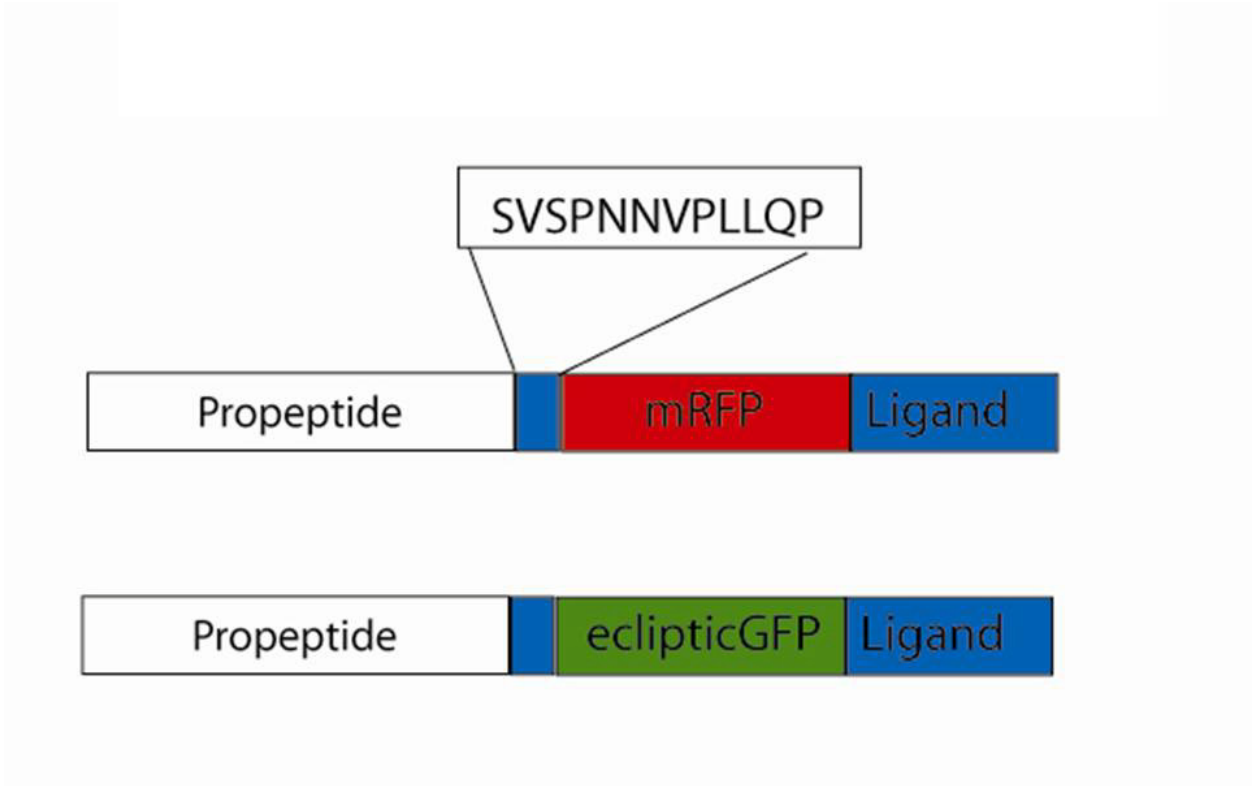

Figure 2.1. **Cloning strategy for Gbb fluorescent protein fusion constructs.** Cartoon shows where fluorescent protein fusions were inserted into the mature ligand domain of Gbb. Box contains the amino acid sequence of the mature ligand domain before insertion of mRFP and superEclipticGFP sequences.

Figure 2.2

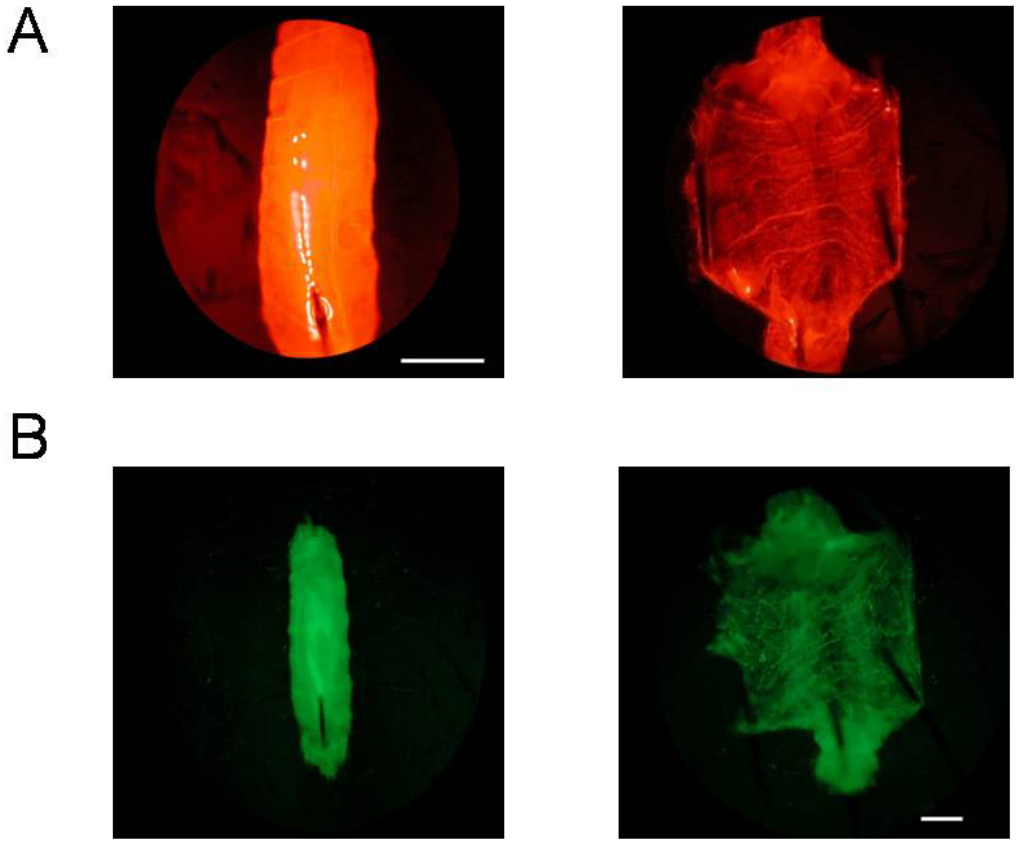

Figure 2.2. Expression of fluorescently tagged Gbb constructs in larvae. (A) Panels show expression of UAS-mRFP-Gbb with 24B-Gal4 driver that expresses in muscles. Expression as observed in intact larva (left) and in dissected larval fillet (right). **(B)** Panels show expression of UAS-superecliptic GFP-Gbb with 24B-Gal4 driver. Expression as observed in intact larva (left) and expression in dissected larval fillet (right). All images were acquired with epifluorescent stereoscope. Scale bars = 1 mm.

Figure 2.3

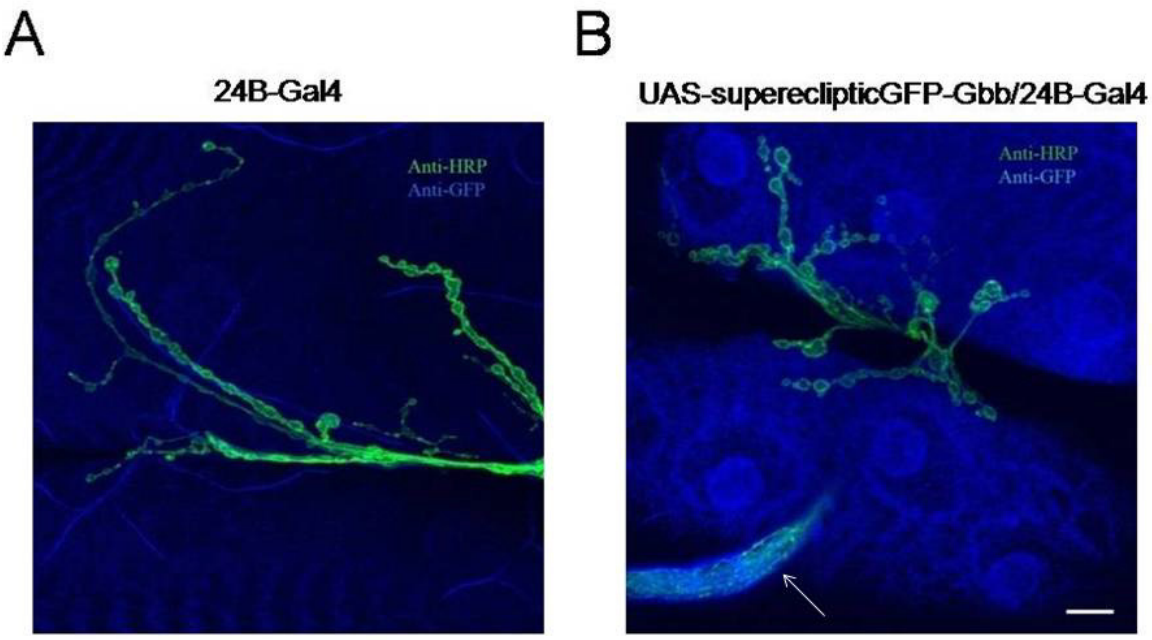

Figure 2.3. Expression of superecliptic GFP-Gbb at NMJs with anti-GFP and anti-HRP antibodies (A) Control NMJ expressing only 24B-Gal4 labeled with antibodies to GFP and HRP **(B)** NMJ expressing UAS-superecliptic GFP/24B-Gal4 labeled with antibodies to GFP and HRP. White arrow points to motor neuron axon that is stained by antibodies to GFP. Scale bar = 20 μm

Figure 2.4

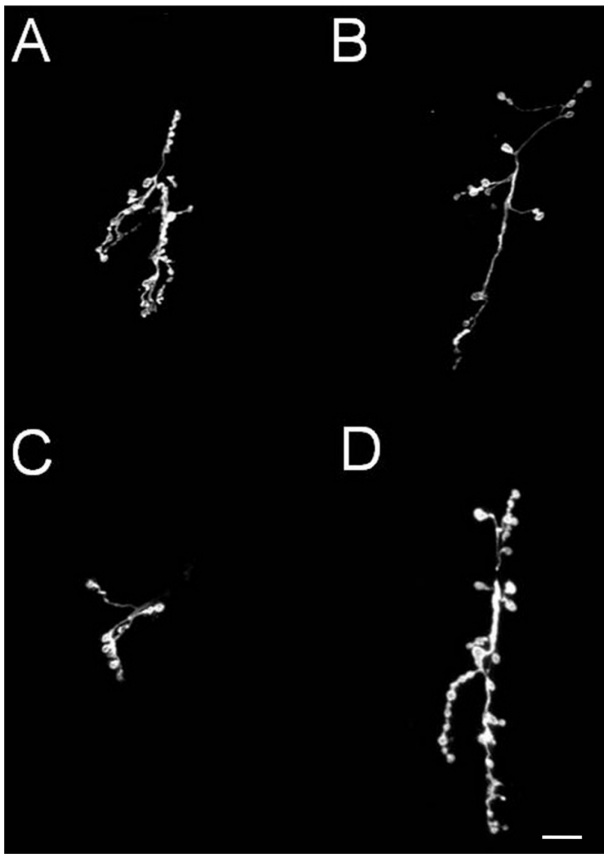
A
B
C
D

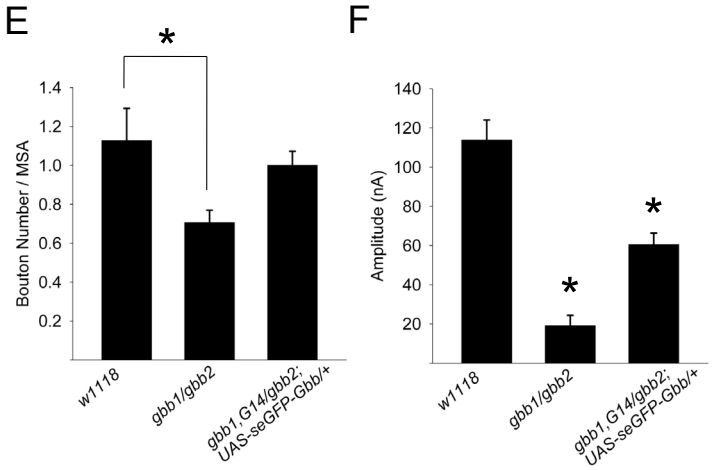
E
F
Bouton Number / MSA
1.4
1.2
1.0
0.8
0.6
0.4
0.2
*
Amplitude (nA)
140
120
100
80
60
40
20
*
*
w1118
gbb1/gbb2
gbb1,G14/gbb2;
UAS-seGFP-Gbb/+

Figure 2.4. Postsynaptic expression of superecliptic GFP-Gbb rescues bouton growth. (A-D) Representative anti-HRP staining of NMJ boutons from different genotypes: (**A)** *w1118* **(B)** *w;gbb1/gbb2;+* **(C)** *w;gbb1,*G14-Gal4*/gbb2;+* **(D)** *w;gbb1,*G14-Gal4*/gbb2;*UAS-ecliptic GFP-Gbb/+ **(E)** Averaged bouton density calculated by bouton number divided by muscle surface area (MSA) for *w1118* (n = 9), *w*;gbb1*/gbb2*;+ (n = 9), and *w;gbb1*,G14/*gbb2*;UAS-superecliptic GFP-Gbb/+ (n = 9). **(F)** Averaged evoked EJC amplitudes for *w1118* (n = 11), *w*;gbb1*/gbb2*;+ (n = 6), and *w;gbb1*,G14/*gbb2*;UAS-superecliptic GFP-Gbb/+ (n = 11). For statistical analysis, multiple comparisons made with one-way anova ($p<0.05$) and Scheffe's test for post hoc analysis ($p<0.05$). Error bars represent SEM. Scale bar = 20 μm.

Figure 2.5

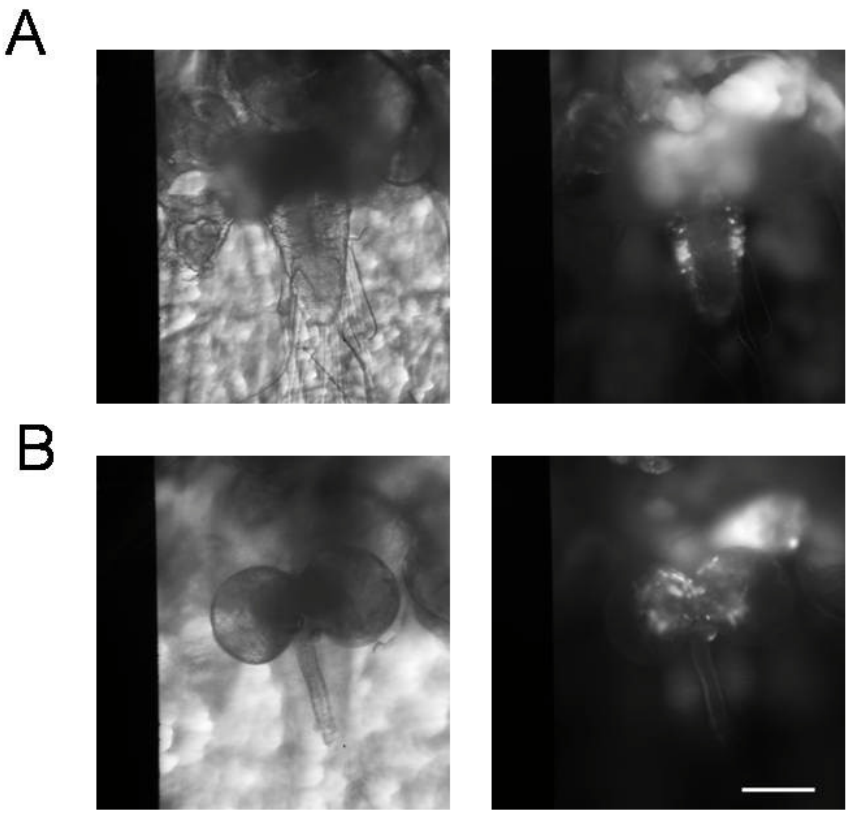

Figure 2.5. **Postsynaptic muscle expression of superecliptic GFP-Gbb results in fluorescence observed in ventral nerve cord and optic lobes. (A)** Images of superecliptic GFP-Gbb expression in larval third-instar dissection. Bright field image of ventral nerve cord (left) and GFP fluorescent image of same ventral nerve cord (right). **(B)** Bright field image of optic lobes (left) and GFP fluorescent image of same optic lobes (right). Scale bar = 0.5 mm.

Figure 2.6

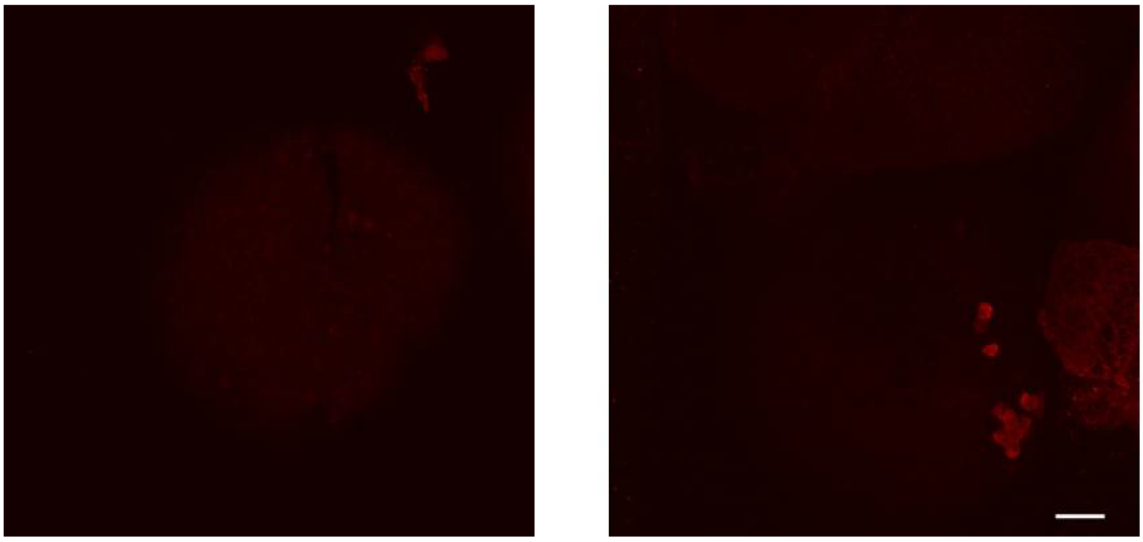

Figure 2.6. Confocal imaging reveals superecliptic GFP-Gbb antibody staining in the optic lobe. Antibody staining using anti-GFP to detect the presence or absence of GFP in the optic lobes. Optic lobe staining from *w*;UAS-GFP;Mef2-Gal4 (left). Optic lobe staining from *w*;UAS-superecliptic GFP-Gbb;Mef2-Gal4 (right). Both preparations were stained under the same treatment. Scale bar = 20 μm.

References

Aberle, H., A. P. Haghighi, et al. (2002). "wishful thinking encodes a BMP type II receptor that regulates synaptic growth in Drosophila." Neuron **33**(4): 545-558.

Baines, R. A. (2004). "Synaptic strengthening mediated by bone morphogenetic protein-dependent retrograde signaling in the Drosophila CNS." J Neurosci **24**(31): 6904-6911.

Ball, R. W., M. Warren-Paquin, et al. (2010). "Retrograde BMP signaling controls synaptic growth at the NMJ by regulating trio expression in motor neurons." Neuron **66**(4): 536-549.

Campbell, R. E., O. Tour, et al. (2002). "A monomeric red fluorescent protein." Proc Natl Acad Sci U S A **99**(12): 7877-7882.

Entchev, E. V., A. Schwabedissen, et al. (2000). "Gradient formation of the TGF-beta homolog Dpp." Cell **103**(6): 981-991.

Marques, G., H. Bao, et al. (2002). "The Drosophila BMP type II receptor Wishful Thinking regulates neuromuscular synapse morphology and function." Neuron **33**(4): 529-543.

McCabe, B. D., G. Marques, et al. (2003). "The BMP homolog Gbb provides a retrograde signal that regulates synaptic growth at the Drosophila neuromuscular junction." Neuron **39**(2): 241-254.

Miesenbock, G., D. A. De Angelis, et al. (1998). "Visualizing secretion and synaptic transmission with pH-sensitive green fluorescent proteins." Nature **394**(6689): 192-195.

O'Connor-Giles, K. M., L. L. Ho, et al. (2008). "Nervous wreck interacts with thickveins and the endocytic machinery to attenuate retrograde BMP signaling during synaptic growth." Neuron **58**(4): 507-518.

Patterson, G. H. and J. Lippincott-Schwartz (2002). "A photoactivatable GFP for selective photolabeling of proteins and cells." Science **297**(5588): 1873-1877.

Teleman, A. A. and S. M. Cohen (2000). "Dpp gradient formation in the Drosophila wing imaginal disc." Cell **103**(6): 971-980.

Wharton, K. A., G. H. Thomsen, et al. (1991). "Drosophila 60A gene, another transforming growth factor beta family member, is closely related to human bone morphogenetic proteins." Proc Natl Acad Sci U S A **88**(20): 9214-9218.

Experimental contributions

Giovanna Guerrero helped with designing Gbb fluorescent fusion constructs and conceiving the initial project. Grant Kauwe helped with designing Gbb fluorescent fusion constructs and experiments using transgenic flies, made the Gbb fluorescent protein fusion constructs, and performed all experiments and analysis. Ehud Isacoff helped design all experiments and supervised the project.

Chapter 3.

Postsynaptic expression of LiGluRs induces synaptic homeostasis at the *Drosophila* NMJ.

Introduction

The *Drosophila* larval neuromuscular junction (NMJ) is a glutamatergic synapse that expresses different types of plasticity, including short-term synaptic plasticity and synaptic homeostasis. Synaptic function can be investigated at the NMJ by using electrophysiology, imaging, and genetic techniques making it a powerful model system for studying synaptic plasticity (Ruiz-Canada and Budnik 2006) . Using genetic manipulations, previous studies have revealed the importance of long-term retrograde signaling for proper synapse function during development (Marques and Zhang 2006).

The Bone Morphogenetic Pathway (BMP) is a major signaling pathway at the NMJ identified by its significant role in synapse development. Much of the work that has elucidated the molecular components of the BMP signaling cascade has relied upon genetic mutant analysis. The putative BMP ligand, Glass Bottom Boat (Gbb), is released from the muscle as a retrograde signal that binds to a presynaptic BMP receptor (McCabe, Marques et al. 2003). This BMP receptor is a heterodimer that consists of Wishful Thinking (Wit), Type II BMP receptor (Aberle, Haghighi et al. 2002; Marques, Bao et al. 2002), and either Type I BMP receptor, Saxophone or Thickveins (McCabe, Hom et al. 2004). Ligand binding to this receptor complex leads to the phosphorylation of Mothers against *dpp* (Mad), a transcription factor, involved in the regulation of genes required for synaptic development (Rawson, Lee et al. 2003). Mad activity regulates the transcription of presynaptic Trio, a Rac guanine exchange factor (Gef), for synaptic growth (Ball, Warren-Paquin et al. 2010). Portions of the BMP signaling pathway are regulated by third-party proteins. Spichthyin (Wang, Shaw et al. 2007) and Nervous Wreck (O'Connor-Giles, Ho et al. 2008) are two negative regulators of BMP signaling that appear to modulate BMP receptor trafficking. In the postsynaptic muscle, the Activin signaling pathway modulates the transcription of Gbb to regulate BMP signaling (Ellis, Parker et al. 2010). Research on various genetic mutants of the components in the BMP signaling cascade revealed that this pathway is critically important in development of the NMJ.

A synaptic homeostatic signal is induced by a mutation in the GluRIIA *Drosophila* glutamate receptor subunit that upregulates synaptic function. A retrograde signal from the muscle instructs the presynaptic neuron to compensate for reduced postsynaptic function by increasing quantal content (Petersen, Fetter et al. 1997). Expression of constitutively active CamKII, a calcium/calmodulin-dependent protein kinase, in muscles prevents the increase in quantal content in the *gluRIIA* mutant. Moreover, the expression of a dominant negative GluRIIA in the muscle does not induce a homeostatic increase in quantal content when coexpressed with the *wit* mutant. Double mutants consisting of *wit* and *gluRIIA* were lethal before third-instar larval stage. These results suggest that CamKII activity and BMP signaling mediate the retrograde signalling that promotes homeostatic synaptic plasticity in *gluRIIA* mutants (Haghighi, McCabe et al. 2003).

The majority of studies on homeostatic synaptic plasticity at the NMJ have investigated the effect of decreased postsynaptic excitability on synaptic function, most often causing an increase in presynaptic quantal content. However, there is less

evidence for the converse homeostatic effect whereby increasing postsynaptic activity eventually leads to a decrease in presynaptic function. Two examples of homeostatic compensation that decrease presynaptic function were found in genetic mutants including larvae with increased muscle innervation (Davis and Goodman 1998) and those with an increase in the glutamate content of presynaptic vesicles (Daniels, Collins et al. 2004). Yet, other manipulations of postsynaptic activity that increase quantal size, including the overexpression of GluRIIA (Petersen, Fetter et al. 1997; Sigrist, Thiel et al. 2002) or the inhibition of postsynaptic PKA (Davis, DiAntonio et al. 1998), do not lead to a compensatory decrease in presynaptic release. One explanation for this discrepancy is that the muscle is monitoring an activity-independent signal from the presynapse to coordinate presynaptic growth with postsynaptic muscle size (Davis and Goodman 1998).

Light Activatable Glutamate Receptors (LiGluRs) are a genetically modified GluR6 kainate receptor that can be photoactivated by 380 nm light and turned off by 500 nm light (Volgraf, Gorostiza et al. 2006). In order to further our understanding of long-term synaptic homeostasis at the NMJ, we decided to express LiGluRs in larval muscles and investigate the effect of chronically increased postsynaptic activity on NMJ development.

Here, we report that the long-term postsynaptic expression of LiGluRs at the NMJ reduces synaptic bouton density and evoked synaptic transmission. Interestingly, postsynaptic LiGluRs do not localize opposite to presynaptic active zones, but instead are located in a perisynaptic region that surrounds presynaptic boutons. Finally, we provide evidence suggesting that LiGluRs at the NMJ primarily respond to spontaneous miniature release but not evoked synaptic transmission. Our results demonstrate that enhanced postsynaptic activity by LiGluR expression activates a retrograde signal to reduce presynaptic function. This could represent a homeostatic mechanism by which NMJs prevent excessive presynaptic growth.

Results and Discussion

Postsynaptic expression of LiGluRs reduces bouton density

To promote enhanced postsynaptic activity during development and observe potential homeostatic changes in synaptic transmission at the NMJ, we made transgenic flies expressing LiGluRs only in the muscle. We took advantage of the GAL4/UAS expression system and generated flies expressing UAS-LiGluR which were crossed to the 24B-Gal4 driver muscle expression line. To examine the expression pattern of LiGluRs at the NMJ of third instar larvae we performed double immunolabeling with a GluR6 antibody, to recognize LiGluRs, and a horseradish peroxidase (HRP) antibody, which serves as a neuronal marker. Surprisingly, postsynaptic LiGluRs localized to the peripheral border of boutons and in the surrounding perisynaptic region (Figure 3.1A).

We next addressed whether or not the long-term postsynaptic expression of LiGluRs alters synapse development at the NMJ. First, we labeled NMJs with

antibodies to HRP and calculated bouton density. We observed a significant decrease in bouton numbers with NMJs expressing LiGluRs as compared to wild-type NMJs (Figure 3.1B-C). We examined control NMJs expressing either 24B-Gal4 or UAS-LiGluR alone and observed normal NMJ development (Figure 3.1D-E). When bouton numbers were normalized to muscle surface area, we observed a significant decrease in bouton density with LiGluR expressing NMJs as compared to wild-type NMJs (Figure 3.1G).

We next wanted to determine whether this decrease in bouton numbers was dependent on channel activity of the LiGluR or whether the physical presence of the receptor at the surface was sufficient to induce this decrease in bouton density. To test this, we generated another transgenic fly line that expresses a low affinity LiGluR containing the K487A mutation which dramatically reduces the affinity of GluR6 for glutamate (Weston, Gertler et al. 2006). When we expressed UAS-LiGluR-Low affinity (LA) along with 24B-Gal4, bouton density was not significantly different from wild-type NMJs ($p = 0.636$) (Figure 3.1F-G). This suggests that there is an increase in postsynaptic activity from LiGluRs responding to endogenous glutamate release during development could bring about homeostatic synaptic plasiticity. Indeed, our results provide evidence that a long-term increase in postsynaptic activity by LiGluR expression triggers retrograde signaling culminating in a compensatory decrease in bouton number.

This intriguing data conflicts with previous attempts which failed to trigger homeostatic compensation by using alternative genetic manipulations to increase postsynaptic activity (Petersen, Fetter et al. 1997; Davis, DiAntonio et al. 1998). It is possible that LiGluRs increase activity above threshold for inducing a retrograde signal while other attempts failed to do so. Another possibility is that LiGluRs localized to the perisynaptic region of the muscle behave differently compared to known *Drosophila* glutamate receptors while being exposed to presynaptic glutamate release. In this way, LiGluR activity could signal independently of known *Drosophila* glutamate receptors at the NMJ, which could explain the discrepancy between our data and other reports.

It is interesting to note that LiGluR expressing NMJs appear to have a significant decrease in bouton density, yet individual boutons appear to be much larger compared to wild-type boutons (Figure 3.1B-C). In the future, it would be important to statistically quantify bouton sizes and determine if there is indeed a significant increase in the size of boutons found in LiGluR expressing NMJs. This could suggest that the decrease in presynaptic growth may not depend on BMP signaling as mutants for the BMP signaling pathway exhibit a significant decrease in bouton density but no change with individual bouton sizes (Marques, Bao et al. 2002; McCabe, Marques et al. 2003).

LiGluRs do not localize opposite to presynaptic active zones

Given that LiGluRs seem to respond to endogenous glutamate release to induce a substantial decrease in presynaptic bouton growth, we next wanted to examine its expression pattern in the postsynaptic muscle. Classically, it has been shown that *Drosophila* glutamate receptors at the NMJ appear as clusters that localize opposite to presynaptic active zones. Antibody staining of the GluRIIA and GluRIIB exchangable

subunits and two of the three essential subunits, GluRIII and GluRIID, indicate that the expression pattern does not differ greatly between subunits (Petersen, Fetter et al. 1997; Marrus, Portman et al. 2004; Featherstone, Rushton et al. 2005; Qin, Schwarz et al. 2005). Based on our initial characterization of LiGluRs at the NMJ, we hypothesize that LiGluR expression does not overlap with presynaptic active zones.

To test this, we performed double immunolabeling experiments using antibodies to Bruchpilot (Brp) which stains active zones (Kittel, Wichmann et al. 2006) and GluR6 to label LiGluRs. When we examined NMJs expressing LiGluRs in the muscle, we observed minimal colocalization between active zones and LiGluR antibody stainings (Figure 3.2A). LiGluRs in the muscle appeared to surround presynaptic active zones and do not show significant colocalization with Bruchpilot staining. Taking this into consideration, we expect that LiGluRs would not colocalize with known *Drosophila* glutamate receptors.

To compare the location of LiGluRs with native *Drosophila* glutamate receptors, we double immunolabled LiGluR expressing NMJs with antibodies against the GluRIIA subunit and LiGluRs. Interestingly, LiGluRs did not colocalize with GluRIIA subunit antibody labeling (Figure 3.2B). This is consistent with our result that LiGluRs are not localized juxtaposed to active zones. Taken together, these results suggest that the retrograde homeostatic signal induced by LiGluR activity at the periphery of the synapse may not be triggered by synaptic glutamate receptors localized directly apposed to active zones.

It is possible that undetectable levels of known *Drosophila* glutamate receptors are located in the perisynaptic region of the muscle occupied by LiGluRs. Similarly, Wit receptors cannot be detected by antibodies at NMJs but is only visualized in motor neuron cell bodies and axons of the CNS. It is thought that either Wit is expressed at extremely low levels at the NMJ or posttranslational modifications mask the epitope target of Wit antibodies (Aberle, Haghighi et al. 2002). However, overexpression of a Wit-GFP construct in neurons results in detection of the Wit receptor at NMJs (unpublished observations, Robin Ball and Guillermo Marques). In the future, we could overexpress the native glutamate receptor subunits and use antibody stains to determine if we achieve greater overlap between *Drosophila* glutamate receptors and LiGluRs. This may provide evidence that known *Drosophila* glutamate receptors do target to regions of the muscle that surrounds boutons and active zones.

An alternative possibility is that LiGluR expression overlaps with unidentified *Drosophila* glutamate receptors. BLAST searches using receptor sequences as queries revealed the presence of five additional candidate genes that could encode for glutamate receptors in the same kainate receptor class as those found at NMJs (Benton, Vannice et al. 2009). It is possible that one or more genes could encode for an unidentified glutamate receptor subunit at the NMJ. It is interesting to note that the GluRIID subunit shares about 37% aminio acid identity with rat, human, and mouse GluR6 receptor, the backbone of LiGluRs. GluRIIE, the *Drosophila* subunit most similar to GluRIID, is 57% identical to GluRIID. The GluRIIA subunit only shares 29% amino acid identity with GluRIID. Additional genes CG5621, CG3822, CG11155, and *clumsy*,

share 49%, 39%, 37%, and 36% respectively, in identity to GluRIID. However, none of these are known to express at NMJs (Featherstone, Rushton et al. 2005). It would be interesting to generate mutants of the unidentified candidate genes that exhibit strong similarities to GluRIID and to clone these genes for construction of fluorescent protein fusion constructs to see if they indeed localize and function at NMJs. It is promising that LiGluRs share strong amino acid similarity with GluRIID and it could suggest that LiGluRs are recapitulating native *Drosophila* functions despite being a mammalian kainate glutamate receptor.

Our observation that LiGluRs are localized at the periphery or region surrounding boutons is reminiscent of Discs Large (Dlg), the *Drosophila* homolog of PSD-95, immunostaining at NMJs. Antibodies to Dlg reveal that it localizes to the border of boutons and surrounds them in a perisynaptic network without significant immunoreactivity in the core of boutons. Dlg staining is found to associate with the postsynaptic subsynaptic reticulum (SSR), a complex system of highly convoluted membranes that surround boutons (Lahey, Gorczyca et al. 1994). As for *Drosophila* glutamate receptors, GluRIIA and GluRIIB staining has been shown to overlap within the area stained by Dlg, however, not all Dlg labeled regions overlap with glutamate receptors (Chen and Featherstone 2005). It would be interesting to do co-immunostaining for LiGluRs and Dlg and determine if their expression at synapses overlaps because this would suggest that LiGluRs may associate with the surrounding SSR.

Postsynaptic expression of LiGluRs reduces presynaptic release probability

We next examined the synaptic physiology of NMJs expressing LiGluR. We conducted miniature excitatory junctional potential (mEJP) recordings from wild-type and LiGluR-expressing NMJs and found that average mEJP frequency and amplitude is not altered as a result of postsynaptic LiGluR expression (Figure 3.3A,C,D). We were surprised that we did not find a decrease in mEJP frequency because we observed a substantial decrease in the number of boutons at NMJs expressing LiGluRs. We postulate that the postsynaptic response of LiGluRs to miniature glutamate release may maintain the number of detected miniature events despite the loss of boutons.

When we recorded single evoked junctional currents (EJCs) from wild-type and LiGluR-expressing NMJs, we found a significant decrease in the average EJC amplitude of NMJs expressing postsynaptic LiGluR compared to wild-type which is consistent with the decrease in synaptic bouton density (Figure 3.3B-E). When we examined release probability by calculating the paired-pulse ratio (PPR), we found a slight, but statistically significant increase in the average PPR with LiGluR expressing NMJs (Figure 3.3B-F). An increase in PPR corresponds to a decrease in presynaptic release probability (Zucker and Regehr 2002). Based on our electrophysiology results, we conclude that postsynaptic expression of LiGluR results in a decrease in evoked synaptic transmission and a decrease in presynaptic release probability.

Acute application of DNQX at LiGluR expressing NMJs reduces spontaneous miniature frequency

We observed a compensatory modification in NMJ structure when we expressed LiGluRs postsynaptically but we did not find a significant change in bouton density at NMJs expressing LiGluRs that have a reduced affinity for glutamate. Therefore, LiGluRs seem to be responding to endogenous glutamate. We wanted to investigate whether LiGluRs participate directly in evoked and/or miniature transmission to induce a homeostatic decrease in the number of boutons. To test this, we used the AMPA glutamate receptor competitive anatagonist, 6,7-dinitroquinoxaline-2,3-dione (DNQX) (Armstrong and Gouaux 2000). DNQX does not significantly block evoked EJPs at the *Drosophila* NMJ (Lee, Bhatt et al. 2009) so we applied DNQX to NMJs in order to block LiGluRs while recording evoked EJCs and mEJPs.

We recorded evoked EJCs and mEJPs before and after the application of 1mM DNQX to determine if LiGluRs do in fact contribute to synaptic transmission. With wild-type NMJs, we did not observe a significant decrease in evoked EJCs as expected when we apply DNQX (Figure 3.4A-B). Similarly, LiGluR expressing NMJs did not exhibit a significant decrease in evoked EJCs with DNQX application (Figure 3.4C-D). These results suggest that LiGluRs do not contribute to evoked synaptic transmission.

We turned our attention to monitoring whether or not mEJP frequency or amplitude are decreased by DNQX application in LiGluR expressing NMJs. Lower DNQX concentrations (250 μM) appeared to reduce the frequency of mEJPs in LiGluR expressing NMJs, and this effect was not observed at wild-type synapses (Figure 3.5). We did not observe a significant change in mEJP amplitudes between LiGluR expressing and wild-type NMJs as a result of DNQX application. This data suggests that LiGluRs are indeed capable of responding to spontaneous miniature release of glutamate at NMJs

It is feasible that we did not see a change in mEJC amplitude because 250 μM DNQX does not sufficiently block LiGluR activity at NMJs. However, it has been shown that 25-100 μM of DNQX is sufficient to block CA1 field potentials when perfused in anesthesized rats (Herreras, Menendez et al. 1989). Thus, we are confident that 250 μM DNQX blocks most if not all LiGluRs at the NMJ during these recordings.

It is surprising that LiGluRs do not respond to evoked glutamate release but only contribute to spontaneous miniature synaptic transmission. It is possible that the perisynaptic localization of LiGluRs could explain their participation only in detection of spontaneous miniature glutamate release. Distinct receptor pools at synapses that are responsive to glutamate depending on the mode of vesicle release (i.e. spontaneous or evoked) have been found. At hippocampal synapses spontaneous miniature and evoked vesicle release activate distinct populations of NMDA receptors (Atasoy, Ertunc et al. 2008). It is possible that the *Drosophila* NMJ could have a similar compartmentalization of its postsynaptic receptors such that one group responds primarily to evoked synaptic transmission and another set may only detect spontaneous miniature glutamate release.

Future experiments

We are very interested in determining the molecular mechanism underlying the synaptic homeostasis induced by postsynaptic LiGluR expression at NMJs. To identify genes that are important for this homeostasis, we propose conducting a genetic screen to mutate genes that block the significant reduction in bouton density found in NMJs that express postsynaptic LiGluRs. In order to quickly assess NMJ growth in mutants from this screen, we can use the fly transgenic line MHC-CD8-GFP-Sh which expresses GFP at postsynapses for *in vivo* analysis of NMJ growth (Zito, Parnas et al. 1999). By conducting a genetic screen, we could gain insight about the retrograde signal and other molecular targets that are important for mediating the significant decrease in boutons at NMJs expressing LiGluRs.

As an additional experiment to demonstrate the requirement of LiGluR activity for inducing synaptic homeostasis at NMJs, we plan to deliver DNQX in food during fly development in order to block LiGluR function. We expect that by blocking LiGluR activity during development we should be able to inhibit the signaling that is necessary to trigger the decrease in bouton numbers. DNQX has been used to block GluR6 activity in hippocampal neuronal cell culture for up to 6 days (Martin, Recasens et al. 2003). Therefore, it is probable that DNQX would be stable in fly food as well. This experiment would provide more evidence that the increased synaptic transmission contributed by LiGluRs activates a homeostatic mechanism for synaptic plasticity.

Figure 3.1

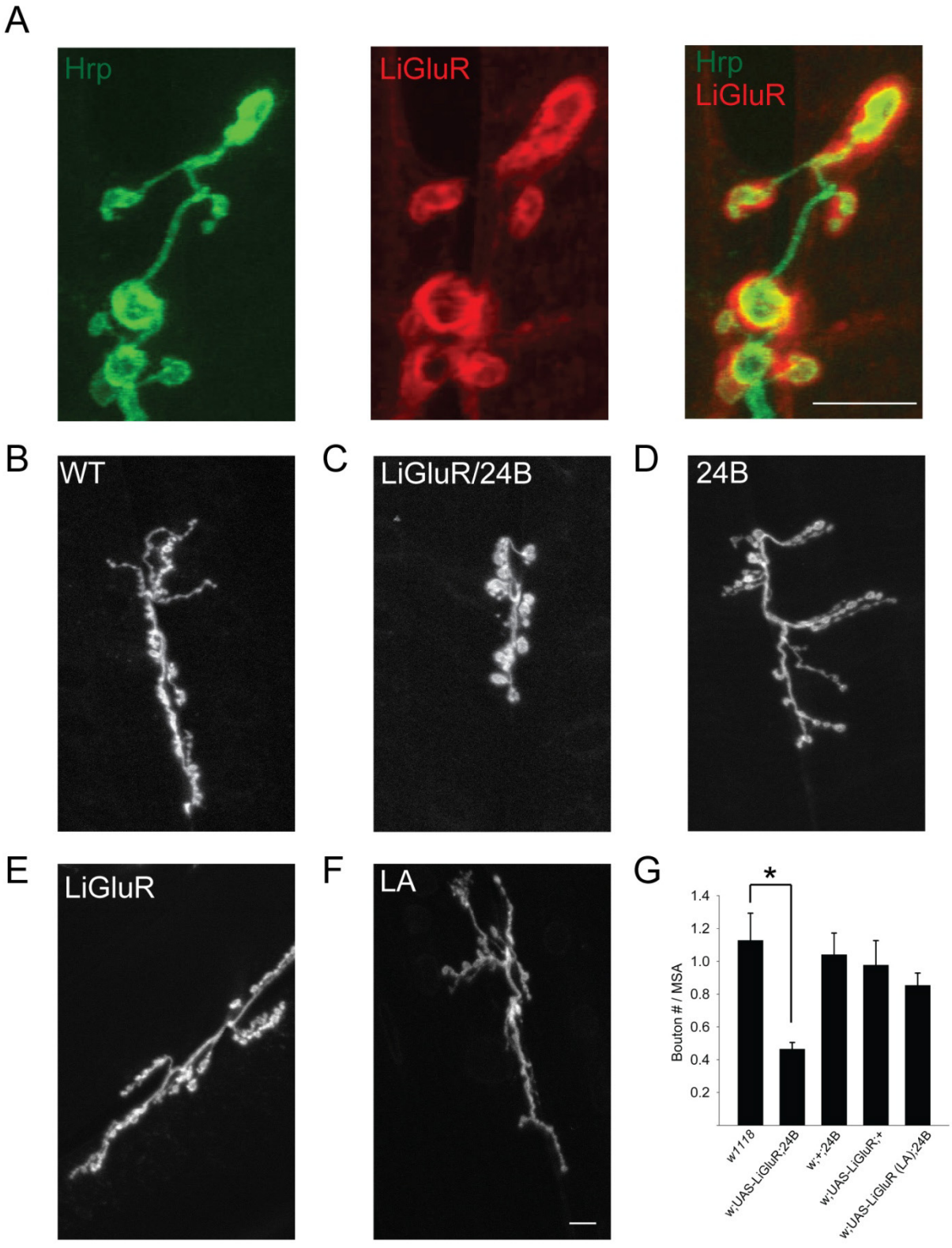
A
Hrp
LiGluR
Hrp
LiGluR
B
WT
C
LiGluR/24B
D
24B
E
LiGluR
F
LA
G
*
Bouton # / MSA
1.4
1.2
1.0
0.8
0.6
0.4
0.2
w1118
w;UAS-LiGluR;24B
w;+;24B
w;UAS-LiGluR;+
w;UAS-LiGluR (LA);24B

Figure 3.1. Postsynaptic expression of LiGluR results in a significant decrease in bouton density.

(A) Third-instar larvae stained with anti-HRP (green) and anti-GluR6 (red) antibodies reveal expression pattern of LiGluRs at NMJs. **(B-F)** Representative antibody stainings using anti-HRP in various genotypes to show that postsynaptic LiGluR expression decreases bouton density: **(B)** *w1118* (n = 9) **(C)** *w*;UAS-LiGluR;24B-Gal4 (n = 9) **(D)** *w*;+;24B-Gal4 (n = 7) **(E)** *w*;UAS-LiGluR;+ (n = 8) **(F)** *w*;UAS-LiGluR(LA);24B-Gal4 (n = 8) **(G)** Graph showing averaged data of bouton density (bouton numbers/muscle surface area) across represented genotypes. For statistical analysis, multiple comparisons made with one-way anova ($p<0.05$) and Scheffe's test for post hoc analysis ($p<0.05$). Bouton density for *w*;UAS-LiGluR;24B-Gal4 is significantly less than *w1118*. Error bars represent SEM. Scale bar = 10 μm.

Figure 3.2

A

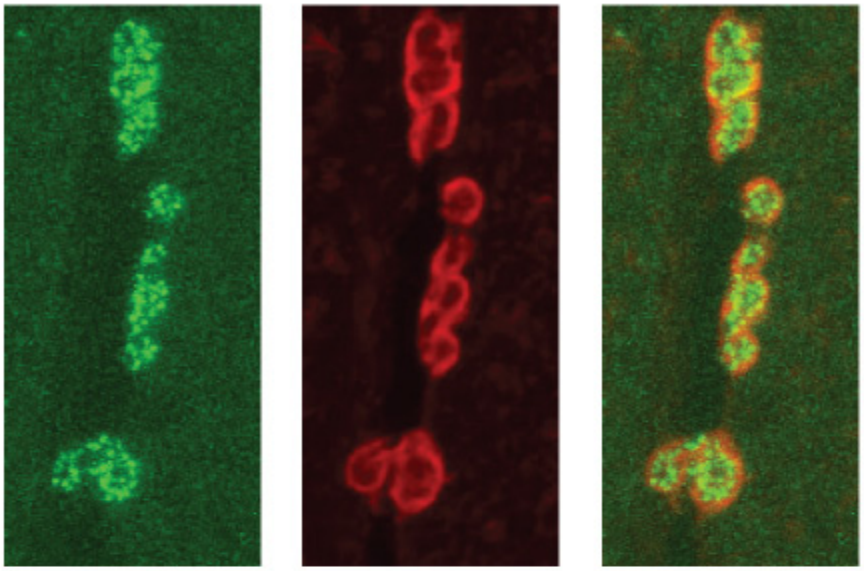

B

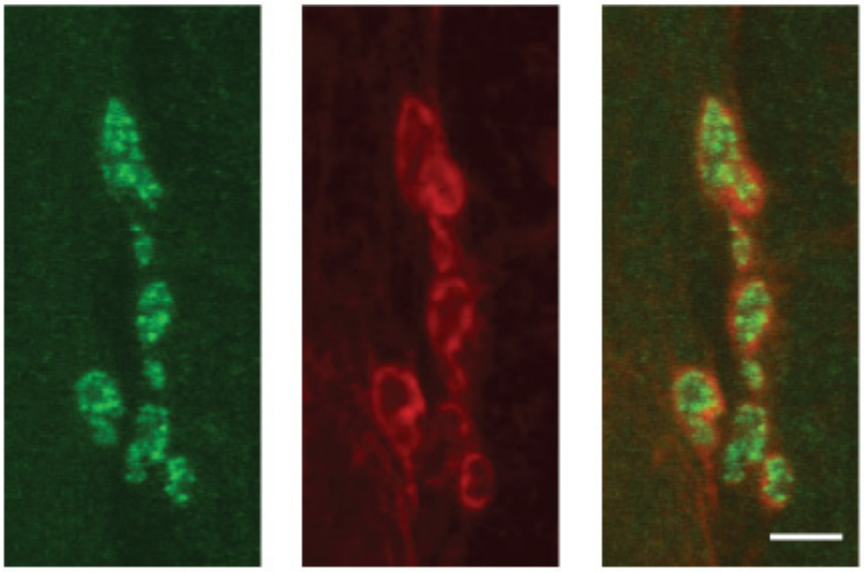

Figure 3.2. LiGluRs do not colocalize opposite to active zones or with GluRIIA subunits.

(A) Confocal images show antibody labeling for Bruchpilot (green) which marks active zones and GluR6 (red) which detects LiGluRs show minimal colocalization. **(B)** Confocal images show antibody labeling for GluRIIA glutamate receptor subunit (green) and GluR6 (red) which exhibit minimal colocalization. LiGluRs appear to surround areas occupied by active zones and *Drosophila* glutamate receptors. Scale bar = 10 μm.

Figure 3.3

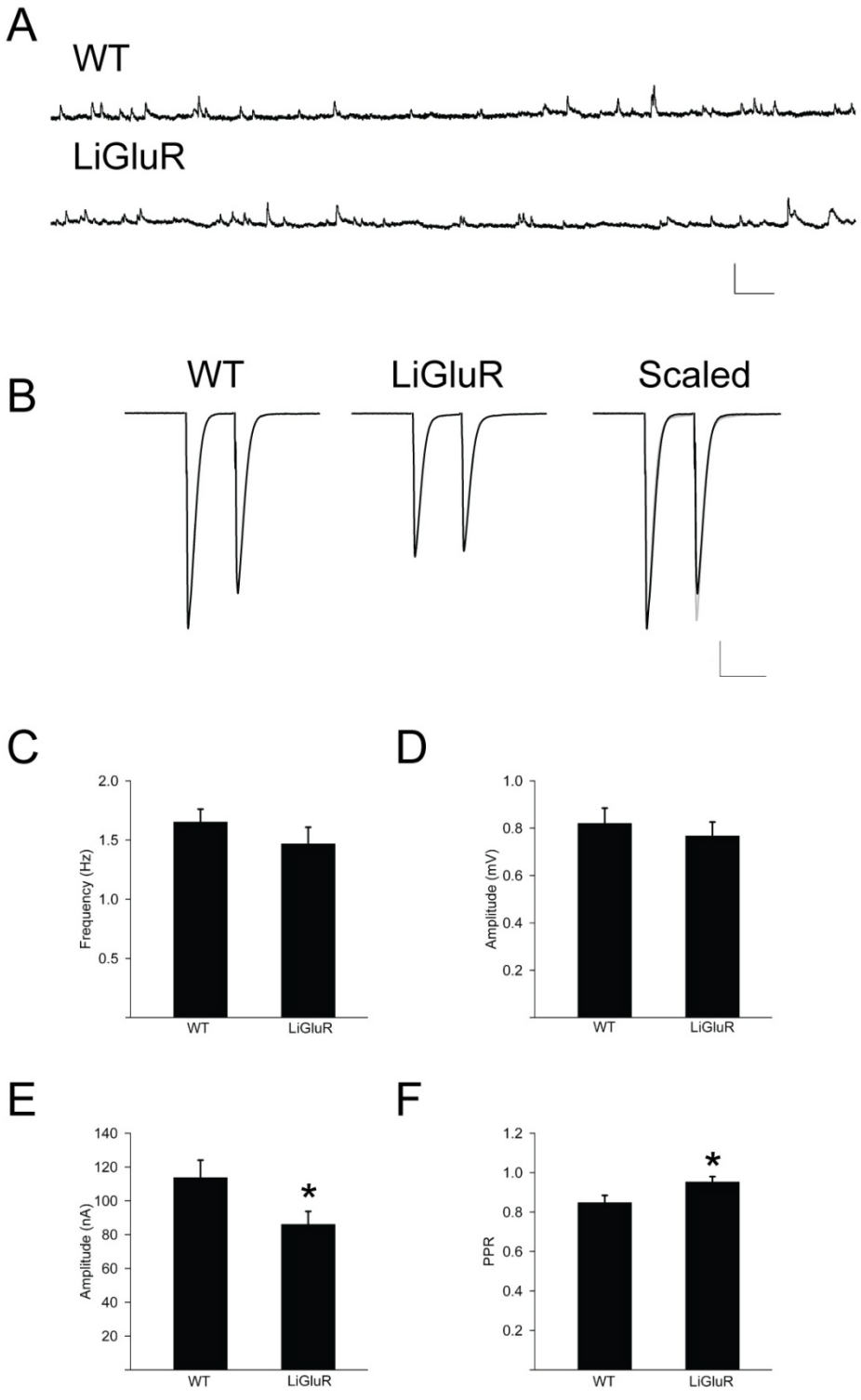
A
WT
LiGluR
B
WT
LiGluR
Scaled
C
Frequency (Hz)
2.0
1.5
1.0
0.5
WT
LiGluR
D
Amplitude (mV)
1.0
0.8
0.6
0.4
0.2
WT
LiGluR
E
Amplitude (nA)
140
120
100
80
60
40
20
*
WT
LiGluR
F
PPR
1.2
1.0
0.8
0.6
0.4
0.2
*
WT
LiGluR

Figure 3.3. Postsynaptic LiGluR expression decreases evoked presynaptic release without a change in mEJP frequency or amplitude.

The genotypes represented by data is *w1118* (WT) and *w;*UAS-LiGluR;24B-Gal4 (LiGluR). **(A)** Representative mEJP traces from 100 second recordings **(B)** Representative paired-pulse traces with 50 ms interpulse interval. Scaled traces have first pulse amplitudes matched between WT and LiGluR in order to better visualize the difference in paired-pulses. **(C-D)** Averaged mEJP frequency data (C) and averaged mEJP amplitude data (D) for WT (n = 11) and LiGluR (n = 9). **(E)** Averaged data across all NMJs for single pulse evoked EJCs for WT (n = 12) and LiGluR (n = 14). For each NMJ, 10 pulses at 0.1 Hz were collected and averaged. LiGluR expressing NMJs exhibit a significant decrease in evoked EJC amplitudes as compared to wild-type NMJs. **(F)** Averaged paired pulse ratio (PPR) (Pulse2/Pulse1) for WT (n = 14) and LiGluR (n = 12). For each NMJ, 10 paired-pulses at 0.1 Hz were recorded with the PPR for each pair calculated, and data was averaged across all 10 paired-pulses. LiGluR expressing NMJs have a statistically significant increase in PPR as compared to wild-type NMJs. The number of samples for each group represents the number of NMJs. For statistical analysis, data was compared with Student's t-test ($p < 0.05$). Scale bar for A is 2 mV and 500 ms. Scale bar for B is 20 nA and 50 ms.

Figure 3.4

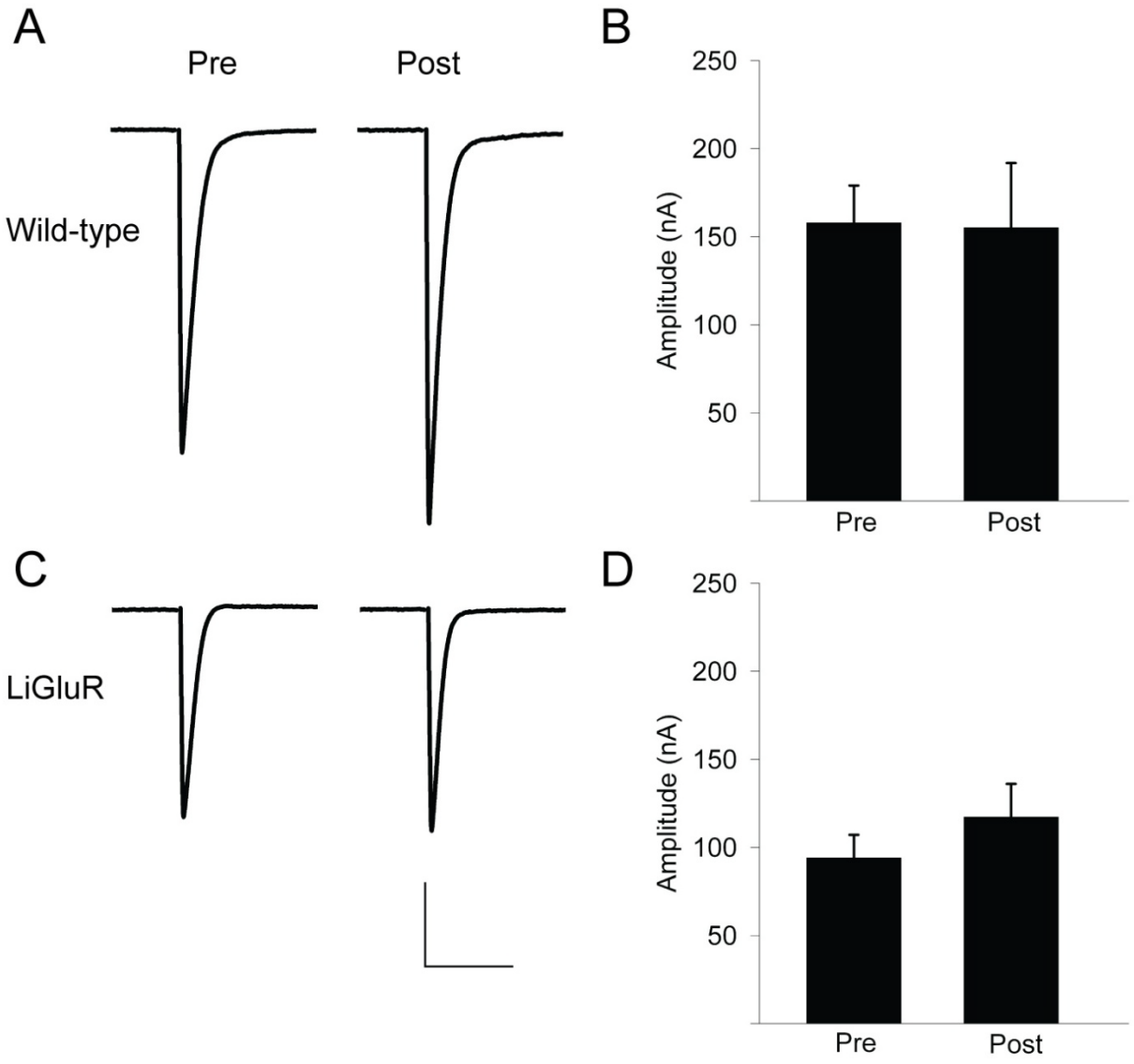
A
Pre
Post
Wild-type
B
250
200
150
100
50
Amplitude (nA)
Pre
Post
C
LiGluR
D
250
200
150
100
50
Amplitude (nA)
Pre
Post

Figure 3.4. Acute DNQX application does not block evoked EJCs in wild-type and LiGluR expressing NMJs.

The genotypes represented by data is *w1118* (WT) and *w;*UAS-LiGluR;24B-Gal4 (LiGluR). For all experiments, 10 evoked EJC pulses at 0.1 Hz were averaged before and after DNQX (1 mM) application. **(A-B)** Representative evoked EJC traces for wild-type NMJs and averaged data for before and after DNQX application (n = 3). **(C-D)** Representative evoked EJC traces for LiGluR expressing NMJs and averaged data for before and after DNQX application (n = 3). For statistical analysis, data was compared with Student's t-test ($p < 0.05$). Scale bar is 50 nA and 50 ms.

Figure 3.5

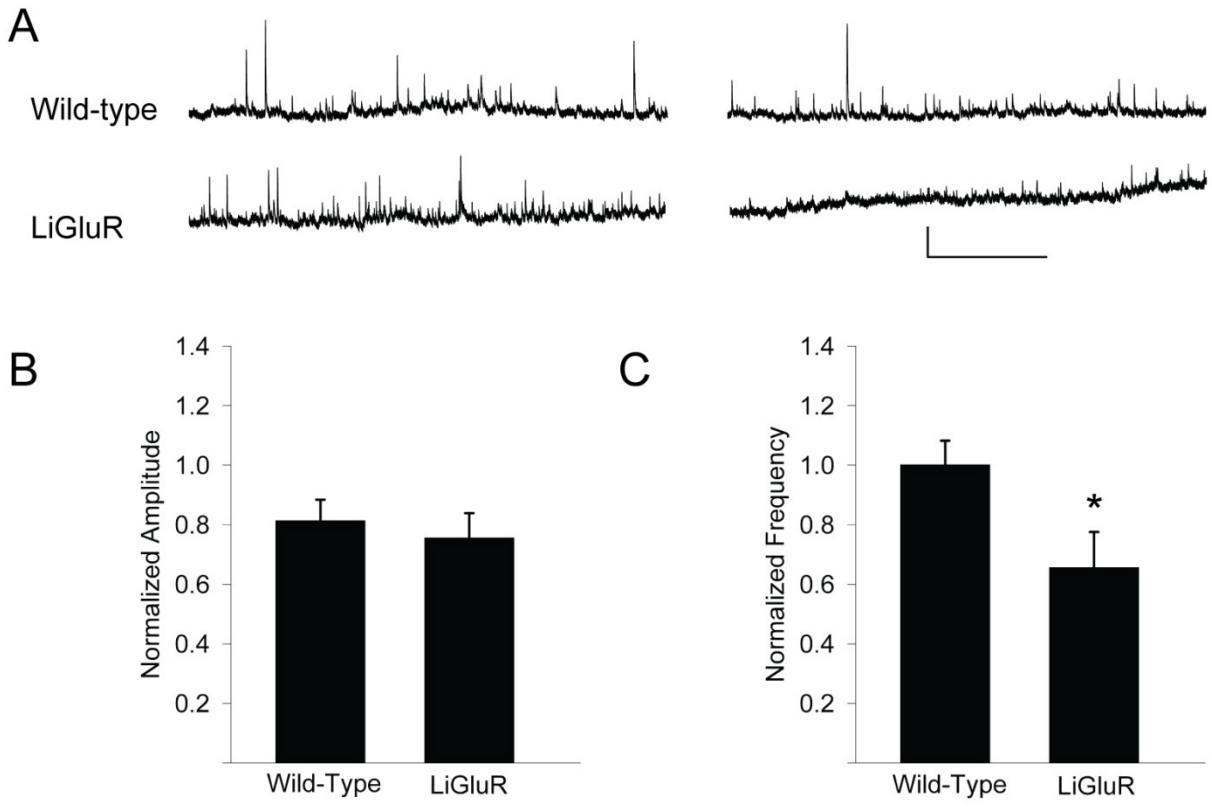

Figure 3.5. Acute DNQX application significantly reduces mEJP frequency in LiGluR expressing NMJs.

The genotypes represented by data is *w1118* (WT) and *w;*UAS-LiGluR;24B-Gal4 (LiGluR). For all experiments, 100 seconds of mEJPs were recorded before and after DNQX (250 μM) application. **(A)** Representative mEJP traces for wild-type and LiGluR expressing NMJs showing data from before DNQX application (left traces) and after DNQX application (right traces). **(B-C)** Averaged normalized data is displayed for mEJP amplitude and frequency after DNQX application. For each NMJ, data is normalized to average baseline mEJP frequency and amplitudes (before DNQX) for WT (n = 3) and LiGluR expressing NMJs (n = 6). For statistical analysis, data was compared with Student's t-test ($p < 0.05$). Scale bar is 1 mV and 5 seconds.

References

Aberle, H., A. P. Haghighi, et al. (2002). "wishful thinking encodes a BMP type II receptor that regulates synaptic growth in Drosophila." Neuron **33**(4): 545-558.

Armstrong, N. and E. Gouaux (2000). "Mechanisms for activation and antagonism of an AMPA-sensitive glutamate receptor: crystal structures of the GluR2 ligand binding core." Neuron **28**(1): 165-181.

Atasoy, D., M. Ertunc, et al. (2008). "Spontaneous and evoked glutamate release activates two populations of NMDA receptors with limited overlap." J Neurosci **28**(40): 10151-10166.

Ball, R. W., M. Warren-Paquin, et al. (2010). "Retrograde BMP signaling controls synaptic growth at the NMJ by regulating trio expression in motor neurons." Neuron **66**(4): 536-549.

Benton, R., K. S. Vannice, et al. (2009). "Variant ionotropic glutamate receptors as chemosensory receptors in Drosophila." Cell **136**(1): 149-162.

Chen, K. and D. E. Featherstone (2005). "Discs-large (DLG) is clustered by presynaptic innervation and regulates postsynaptic glutamate receptor subunit composition in Drosophila." BMC Biol **3**: 1.

Daniels, R. W., C. A. Collins, et al. (2004). "Increased expression of the Drosophila vesicular glutamate transporter leads to excess glutamate release and a compensatory decrease in quantal content." J Neurosci **24**(46): 10466-10474.

Davis, G. W., A. DiAntonio, et al. (1998). "Postsynaptic PKA controls quantal size and reveals a retrograde signal that regulates presynaptic transmitter release in Drosophila." Neuron **20**(2): 305-315.

Davis, G. W. and C. S. Goodman (1998). "Genetic analysis of synaptic development and plasticity: homeostatic regulation of synaptic efficacy." Curr Opin Neurobiol **8**(1): 149-156.

Davis, G. W. and C. S. Goodman (1998). "Synapse-specific control of synaptic efficacy at the terminals of a single neuron." Nature **392**(6671): 82-86.

Ellis, J. E., L. Parker, et al. (2010). "Activin signaling functions upstream of Gbb to regulate synaptic growth at the Drosophila neuromuscular junction." Dev Biol **342**(2): 121-133.

Featherstone, D. E., E. Rushton, et al. (2005). "An essential Drosophila glutamate receptor subunit that functions in both central neuropil and neuromuscular junction." J Neurosci **25**(12): 3199-3208.

Haghighi, A. P., B. D. McCabe, et al. (2003). "Retrograde control of synaptic transmission by postsynaptic CaMKII at the Drosophila neuromuscular junction." Neuron **39**(2): 255-267.

Herreras, O., N. Menendez, et al. (1989). "Synaptic transmission at the Schaffer-CA1 synapse is blocked by 6,7-dinitro-quinoxaline-2,3-dione. An in vivo brain dialysis study in the rat." Neurosci Lett **99**(1-2): 119-124.

Kittel, R. J., C. Wichmann, et al. (2006). "Bruchpilot promotes active zone assembly, Ca2+ channel clustering, and vesicle release." Science **312**(5776): 1051-1054.

Lahey, T., M. Gorczyca, et al. (1994). "The Drosophila tumor suppressor gene dlg is required for normal synaptic bouton structure." Neuron **13**(4): 823-835.

Lee, J. Y., D. Bhatt, et al. (2009). "Furthering pharmacological and physiological assessment of the glutamatergic receptors at the Drosophila neuromuscular junction." Comp Biochem Physiol C Toxicol Pharmacol **150**(4): 546-557.

Marques, G., H. Bao, et al. (2002). "The Drosophila BMP type II receptor Wishful Thinking regulates neuromuscular synapse morphology and function." Neuron **33**(4): 529-543.

Marques, G. and B. Zhang (2006). "Retrograde signaling that regulates synaptic development and function at the Drosophila neuromuscular junction." Int Rev Neurobiol **75**: 267-285.

Marrus, S. B., S. L. Portman, et al. (2004). "Differential localization of glutamate receptor subunits at the Drosophila neuromuscular junction." J Neurosci **24**(6): 1406-1415.

Martin, A., M. Recasens, et al. (2003). "DNQX-induced toxicity in cultured rat hippocampal neurons: an apparent AMPA receptor-independent effect?" Neurochem Int **42**(3): 251-260.

McCabe, B. D., S. Hom, et al. (2004). "Highwire regulates presynaptic BMP signaling essential for synaptic growth." Neuron **41**(6): 891-905.

McCabe, B. D., G. Marques, et al. (2003). "The BMP homolog Gbb provides a retrograde signal that regulates synaptic growth at the Drosophila neuromuscular junction." Neuron **39**(2): 241-254.

O'Connor-Giles, K. M., L. L. Ho, et al. (2008). "Nervous wreck interacts with thickveins and the endocytic machinery to attenuate retrograde BMP signaling during synaptic growth." Neuron **58**(4): 507-518.

Petersen, S. A., R. D. Fetter, et al. (1997). "Genetic analysis of glutamate receptors in Drosophila reveals a retrograde signal regulating presynaptic transmitter release." Neuron **19**(6): 1237-1248.

Qin, G., T. Schwarz, et al. (2005). "Four different subunits are essential for expressing the synaptic glutamate receptor at neuromuscular junctions of Drosophila." J Neurosci **25**(12): 3209-3218.

Rawson, J. M., M. Lee, et al. (2003). "Drosophila neuromuscular synapse assembly and function require the TGF-beta type I receptor saxophone and the transcription factor Mad." J Neurobiol **55**(2): 134-150.

Ruiz-Canada, C. and V. Budnik (2006). "Introduction on the use of the Drosophila embryonic/larval neuromuscular junction as a model system to study synapse development and function, and a brief summary of pathfinding and target recognition." Int Rev Neurobiol **75**: 1-31.

Sigrist, S. J., P. R. Thiel, et al. (2002). "The postsynaptic glutamate receptor subunit DGluR-IIA mediates long-term plasticity in Drosophila." J Neurosci **22**(17): 7362-7372.

Volgraf, M., P. Gorostiza, et al. (2006). "Allosteric control of an ionotropic glutamate receptor with an optical switch." Nat Chem Biol **2**(1): 47-52.

Wang, X., W. R. Shaw, et al. (2007). "Drosophila spichthyin inhibits BMP signaling and regulates synaptic growth and axonal microtubules." Nat Neurosci **10**(2): 177-185.

Weston, M. C., C. Gertler, et al. (2006). "Interdomain interactions in AMPA and kainate receptors regulate affinity for glutamate." J Neurosci **26**(29): 7650-7658.

Zito, K., D. Parnas, et al. (1999). "Watching a synapse grow: noninvasive confocal imaging of synaptic growth in Drosophila." Neuron **22**(4): 719-729.

Zucker, R. S. and W. G. Regehr (2002). "Short-term synaptic plasticity." Annu Rev Physiol **64**: 355-405.

Experimental Contributions

Gautam Agarwal cloned LiGluR into pUAST fly vector and injected the construct into embryos. Stephanie Szobota made low affinity LiGluR mutant and Zhu Fu cloned LiGluR into pUAST vector. Grant Kauwe helped with designing experiments and performed all experiments and analysis. Ehud Isacoff helped design all experiments and supervised the project.

Chapter 4

Effect of acute LiGluR activation on synaptic strength

Introduction

Recent reports suggest that a retrograde signal from the postsynaptic muscle at *Drosophila* NMJs can rapidly increase presynaptic strength within minutes (Yoshihara, Adolfsen et al. 2005; Frank, Kennedy et al. 2006). Application of philanthotoxin, a non-competitive glutamate antagonist, blocks postsynaptic glutamate receptors causing an immediate reduction in evoked EJP and mEJP amplitudes which triggers a retrograde signal to increase presynaptic quantal content within ten minutes. The evoked EJP amplitude is restored to nearly baseline levels. This rapid induction of synaptic homeostasis does not require protein synthesis, evoked neurotransmission, or activity from the motoneuron soma (Frank, Kennedy et al. 2006). Mutants of components in the BMP signaling pathway, including *wit, mad,* and *gbb,* block the compensatory recovery of evoked EJP amplitude. Interestingly, neuronal or muscle expression of Gbb both restore signaling for rapid synaptic homeostasis in the *gbb* mutant. BMP signaling through Wit and Gbb may confer competency in motoneurons for synaptic homeostasis to occur during larval development. Since the motoneuron cell body is not required for rapid induction of synaptic homeostasis, this suggests that Gbb may not be the instructive signal at the NMJ (Goold and Davis 2007).

Another form of rapid retrograde signaling at the NMJ is regulated by Syt 4, the synaptotagmin 4 isoform that is localized at postsynaptic sites of the muscle. Stimulating embryonic or third-instar laval NMJs for 1 minute at 100 Hz induces a high frequency miniature release that is blocked in the *syt 4* mutant (Yoshihara, Adolfsen et al. 2005; Barber, Jorquera et al. 2009). Injection of the calcium chelator 1,2-bis(2-aminophenoxy)ethane-N,N,N',N'-tetraacetic acid (BAPTA) into the muscle of embryonic NMJs suppresses the induction of high frequency miniature release. This suggests that Ca^{2+}-dependent release of a retrograde signal from the postsynapse is required for this potentiation of presynaptic function mediated by Syt 4 activity (Yoshihara, Adolfsen et al. 2005).

Despite these two findings demonstrating that rapid retrograde signaling occurs at the NMJ, there are remaining questions left unanswered. We do not know the identity of the retrograde signal, its exact time course, or how long it persists. In addition to this, we do not have a clear understanding of the relationship between different forms of synaptic plasticity mediated by retrograde signaling at the NMJ namely both homeostasic mechanisms and synaptic potentiation. Finally, Syt 4-dependent retrograde signaling manifests itself during extremely high frequency stimulation, however, we do not know if it plays a role during lower frequency stimulation as well.

To further address the mechanisms underlying the rapid induction of synaptic plasticity at the *Drosophila* NMJ, we used larvae expressing the Light Activatable Glutamate Receptors (LiGluRs) specifically in the muscle. The LiGluRs can be used as a tool to rapidly increase postsynaptic activity (Szobota, Gorostiza et al. 2007). We previously used LiGluRs to study the effects of a chronic increase in postsynaptic activity (Chapter 3), and here we can take advantage of the photoswitching capabilities

of LiGluRs to selectively alter postsynaptic activity on a rapid time scale. Application of the photoswtichable ligand, Maleimide-Azobenzene-Glutamate (MAG), enables the activation of LiGluRs with 380 nm light and their inactivation with 500 nm light (Figure 4.1A) (Volgraf, Gorostiza et al. 2006). This method allows for the precise temporal and spatial control of postsynaptic activity.

Here we report that within five minutes of acute postsynaptic LiGluR activation the depression of synaptic responses normally observed during high frequency trains is alleviated, thereby signifying a strengthening of synaptic transmission. This synaptic plasticity appears to require postsynaptic CamKII activity and cAMP signaling. However, it does not require BMP signaling through the presynaptic Wit receptor. Our results suggest that we have uncovered a retrograde signaling pathway important for rapidly potentiating synaptic transmission in response to an acute increase postsynaptic activity.

Results and Discussion

LiGluRs can be photoactivated at NMJs

We found that postsynaptic LiGluRs are specifically expressed in the perisynaptic region surrounding boutons. Furthermore, we demonstrated that long-term expression of LiGluRs at NMJs induces a homeostatic decrease in presynaptic bouton density and evoked synaptic transmission (Chapter 3). Therefore, LiGluRs are efficiently trafficked to the surface and they are functional at the NMJ. We next wondered whether or not acute LiGluR activation could promote synaptic plasticity. It is possible that LiGluR activation could trigger a compensatory decrease in presynaptic function similar to the rapid homeostatic response reported albeit in the reverse direction (Frank, Kennedy et al. 2006). Alternatively, increased postsynaptic activity could signal a positive feedback mechanism to potentiate presynaptic vesicle release (Yoshihara, Adolfsen et al. 2005). To explore these possibilities, we turned to photoswitching experiments for precise temporal control of LiGluR activity.

LiGluRs are photoswitched by MAG which contains an azobenzene optical switch. In the *cis* state, MAG delivers tethered glutamate to the binding pocket with 380 nm light and in the *trans* state, MAG removes glutamate from the binding pocket upon illumination with 500 nm light (Volgraf, Gorostiza et al. 2006) (Figure 4.1A). To photoswitch LiGluRs, we exogenously introduced MAG in dissected third-instar larva fillets. We labeled in low calcium (0.45 mM Ca^{++}) hemolymph-like solution (HL3) to prevent spontaneous muscle contractions. In our recording solution, we added Thapsigargin, to block muscle contractions (Guerrero, Reiff et al. 2005), and Concanavalin A to block desensitization of LiGluRs (Partin, Patneau et al. 1993). When we tested the photoswitching of LiGluRs, an inward current was observed with 380 nm light that continued after turning off the light source. This inward current was deactivated with illumination of 500 nm light (Figure 4.1B). The continuous LiGluR inward current after removal of 380 nm light is a property of the azobenzene photoswitch slowly relaxing into the *trans* (inactive) state in the dark (Gorostiza and

Isacoff 2008). After demonstrating the efficacy and reliability of LiGluR photoswtiching at NMJs, we continued with experiments to examine synaptic strength following acute postsynaptic activation.

In initial experiments, we recorded mEJPs before and after five minutes of LiGluR activation. We did not observe any change in mEJP frequency or amplitude as a result of enhanced postsynaptic activity (Figures 4.1C and D). Paired-pulse ratio (PPR) is inversely related to the synaptic release probability (Zucker and Regehr 2002) and it is a commonly used method to assess presynaptic function. The PPR was calculated from the postsynaptic responses to pairs of stimuli administered at 0.1 Hz. The PPR was measured before and after five minutes of LiGluR activation in control NMJs which were treated with MAG but did not receive light and NMJs that received LiGluR activation. We did not observe any differences in PPR as a result of LiGluR activity (Figure 4.1E). This suggests that an acute enhancement in postsynaptic activity by LiGluRs does not change mEJPs and the synaptic release probability.

Postsynaptic LiGluRs enhance evoked synaptic transmission during high frequency trains

Another method to evaluate synaptic function is to monitor the rate of presynaptic vesicle depletion during high frequency stimulation (Dobrunz and Stevens 1997). In a presynaptic bouton there are two pools of synaptic vesicles, the recycling pool that supplies vesicles to maintain basal synaptic transmission and the reserve pool of vesicles that are recruited during high frequency stimulation (Kuromi and Kidokoro 1998). We examined the efficacy of synaptic transmission during high frequency stimulation with and without postsynaptic LiGluR activation. We stimulated NMJs at 20 Hz for 1 second (60 seconds between trains) and normalized each postsynaptic response to the average amplitude of baseline EJCs taken for each NMJ (Figure 4.2A). We performed a control experiment in which NMJs were treated with MAG but were not exposed to light and an experiment in which NMJs were treated with MAG and light. Before LiGluR activation, the first five responses to high frequency stimulation were not different between both groups (Figure 4.2B left panel). However, after LiGluR activation, we observed a significant difference in the amplitude of the first five responses to high frequency stimulation (Figures 4.2B-D). Surprisingly, acute LiGluR activation increased the amplitude of the evoked postsynaptic response during train stimulation compared to controls. This attenuation of synaptic depression is consistent with an increase in availability of vesicles for release during high frequency transmission; likely due to the enhanced recruitment of vesicles from the reserve pool. Here, we provide evidence that acute postsynaptic LiGluR activation alters synaptic strength by potentiating the response to high frequency stimulation.

Postsynaptic CamKII activity is required for synaptic enhancement induced by postsynaptic LiGluR activation

We were interested in determining whether postsynaptic Ca^{2+}/Calmodulin-dependent protein kinase II (CamKII) is required for the increase in synaptic strength

induced by LiGluR activity. In mammalian synapses, postsynaptic CamKII plays a role in long-term potentiation (LTP) through phosphorylation of AMPA receptors (AMPARs) (Barria, Muller et al. 1997; Lee, Barbarosie et al. 2000) and insertion of AMPARs into existing synapses (Hayashi, Shi et al. 2000; Poncer, Esteban et al. 2002). At the *Drosophila* NMJ, postsynaptic inhibition of CamKII induces a compensatory increase in presynaptic quantal content and constitutively active postsynaptic CamKII inhibits the retrograde signal induced in the *glurIIA* mutant (Haghighi, McCabe et al. 2003). In newly hatched first-instar larvae, expression of constitutively active postsynaptic CamKII enhances the area of presynaptic boutons, the amount of presynaptic Synaptotagmin I immunostaining, and the area of postsynaptic GluRIIA expression (Kazama, Morimoto-Tanifuji et al. 2003). This effect is specific to early first-instar larval NMJs as expression of constitutively active postsynaptic CamKII in third-instar larval NMJs reduces presynaptic quantal content without a change in quantal size (Haghighi, McCabe et al. 2003).

To determine if CamKII activity is required for synaptic plasticity in response to LiGluR activity, we expressed a peptide corresponding to the rat autoinhibitory domain of CamKII with the T286A mutation (Griffith, Verselis et al. 1993) in larval muscles (Haghighi, McCabe et al. 2003). First, we examined the effect of postsynaptic inhibition of CamKII on the homeostatic decrease in bouton density triggered by chronic LiGluR activity throughout development.

We used horseradish peroxidase (HRP) antibodies (Chapter 3) to label presynaptic boutons and found that postsynaptic inhibition of CamKII during development does not block the LiGluR induced decrease in bouton density (Figures 4.3A and C). Interestingly, we did observe a marginal increase in evoked EJC amplitudes with NMJs expressing the CamKII inhibitory peptide together with LiGluRs (Figures 4.3B and D). This is consistent with the observation that postsynaptic CamKII inhibition during development leads to a homeostatic increase in evoked EJP amplitude (Haghighi, McCabe et al. 2003). In summary, our results suggest that inhibition of postsynaptic CamKII does not inhibit the structural homeostatic compensation induced by chronic LiGluR activity. However, the homeostatic signal induced by postsynaptic CamKII inhibition could account for the increase in evoked EJC amplitude that we observe despite LiGluR expression. These results indicate that postsynaptic inhibition of CamKII is not required for the synaptic homeostasis induced by long-term postsynaptic expression of LiGluRs.

Next, we monitored the depletion of synaptic vesicles by high frequency stimulation following LiGluR activation in larvae expressing the CamKII inhibitory peptide in the muscle. If CamKII is involved in the signaling pathway to strengthen synaptic function following LiGluR activation, then we would expect to find normal synaptic depression with CamKII inhibition. Before LiGluR activation, we did not observe any change in the amplitude of the first five responses to the high frequency train with the postsynaptic expression of CamKII inhibitory peptide (Figure 4.3E). However, after LiGluR activation, we did not observe a potentiation of responses from NMJs expressing the CamKII inhibito, instead the depression of synaptic transmission

was similar to control NMJs (Figure 4.3F). This indicates that inhibition of postsynaptic CamKII activity blocks the potentiating effect of LiGluR activity on synaptic transmision and suggests a role for postsynaptic CamKII in mediating the rapid LiGluR-induced change in synaptic strength.

Wishful Thinking BMP receptor is not required for LiGluR induced synaptic enhancement

We next wondered whether BMP signaling plays a role in the synaptic potentiation observed following postsynaptic LiGluR activation. To test this, we expressed LiGluRs in the *wit* mutant background. We could not assess synaptic function with high frequency stimulation because the extreme deficit in synaptic transmission in the *wit* mutant led to failures of evoked synaptic transmission within initial trains (data not shown) (Aberle, Haghighi et al. 2002; Marques, Bao et al. 2002). To circumvent this problem, we applied continuous paired-pulse stimulation at 0.1 Hz before, during, and after LiGluR activation. We found that this lower frequency stimulation protocol does not depress *wit* mutant synapses as quickly as the high frequency trains.

First, we wanted to verify that acute LiGluR activation could potentiate synaptic transmission during this modified stimulation protocol. For each recording, we normalized the amplitude of paired-pulse responses to baseline EJC amplitudes and we monitored the average amplitude of every ten paired-pulse responses. When we analyzed the normalized amplitude of the first response to paired stimulation, we observed a rapid enhancement of synaptic transmission after LiGluR activation compared to the control (Figure 4.4A). These results are consistent with our previous findings that demonstrated enhancement of synaptic transmission during high frequency stimulation and indicates that LiGluRs are indeed capable of altering synaptic strength in the context of this new stimulation protocol.

Moving forward, we used the paired-pulse stimulation protocol to monitor synaptic function at NMJs expressing LiGluRs in the *wit* mutant background. When we performed the paired-pulse stimulation protocol, our initial results revealed a trend in enhanced synaptic function with *wit* mutant NMJs receiving LiGluR activation (Figure 4.4B). We also tested the effect of acute LiGluR activation in the *wit* mutant with an alternative paired-pulse protocol that shows synaptic potentiation (Figure A.2). If these results hold, it would indicate that the Wit receptor is not required for the LiGluR-induced alteration of synaptic strength and suggests that Wit-dependent BMP signaling is not involved. As an additional experiment, we attempted to express LiGluRs in the *gbb* mutant background, but failed to recover any third-instar larvae.

We next wanted to investigate the molecular mechanism involved with the LiGluR-induced enhancement of synaptic strength during high frequency stimulation. At *Drosophila* NMJs, two distinct vesicle pools exist: the exo/endo cycling pool and the reserve pool (Kuromi and Kidokoro 1998). Experiments demonstrated that cAMP-PKA signaling is important for mobilization of vesicles from the reserve pool to the exo/endo

cycling pool during high frequency stimulation for vesicular release of glutamate (Kuromi and Kidokoro 2000). Since we observed an attenuation of synaptic depression following LiGluR activation which suggests an increase in the availability of synaptic vesicles for release, we wondered whether cAMP signaling is involved.

To test this hypothesis, we used acute treatment of db-cAMP, a membrane permeable cAMP analog, and rp-cAMPs, a membrane permeable cAMP competitive antagonist, to alter cAMP signaling at the NMJ during the high frequency stimulation protocol. First, we examined the effect of db-cAMP treatment on synaptic transmission during high frequency stimulation in larvae expressing LiGluR but without acute LiGluR activation. Indeed, similar to previous work we found an attenuation of synaptic vesicle depletion in the presence of db-cAMP (Figures 4.4C and D) (Kuromi and Kidokoro 2000). We observed a similar effect upon acute postsynaptic LiGluR activation raising the possibility that LiGluR activity triggers a retrograde signal to rapidly increase cAMP levels leading to enhanced synaptic vesicle release. Next, we used rp-cAMPs treatment during LiGluR activation to see if antagonism of the cAMP signaling pathway can block the potentiaion of synaptic transmission during high frequency stimulation. Interestingly, LiGluR activation did not alter synaptic depression with rp-cAMPs treatment (Figures 4.4E and F). These results suggest that the mechanism underlying the potentiation induced by acute LiGluR activation could involve cAMP signaling which is known to recruit vesicles from the reserve pool during high frequency synaptic transmission.

Future experiments

Our experiments showed that acute LiGluR activation of the postsynaptic muscle enhances synaptic transmission during high frequency stimulation. Postsynaptic CamKII activity is required for the attenuation of synaptic depression during high frequency stimulation and it is likely that BMP signaling is not involved. Finally, we have evidence that implicates presynaptic cAMP signaling in the synaptic potentiation generated by acute LiGluR activation.

We recognize that more experiments should be done to confirm these findings. We need to complete more recordings for the *wit* mutant experiments to determine if BMP signaling is required for the LiGluR dependent potentiation. To further investigate the potential role of cAMP signaling in LiGluR induced potentiaion, we can establish whether or not db-cAMP occludes the LiGluR effect by performing high frequency stimulation experiments with LiGluR activation and db-cAMP treatment. If application of db-cAMP during postsynaptic LiGluR activation leads to an even greater synaptic potentiation, this would indicate that LiGluR activation and cAMP signaling modify synaptic transmission through two parallel mechanisms. In the presence of db-cAMP, if there is no further potentiation with LiGluR activation, then this would indicate that db-cAMP occludes the LiGluR dependent plasticity. In addition, we need to perform control experiments using rp-cAMPs treatment without LiGluR activation to determine whether or not synaptic depression is altered by the blockade of cAMP signaling. To complement these cAMP experiments, we can treat NMJs with cytochalasin D, which

eliminates the reserve pool without affecting the exo/endo cycling pool, and determine whether LiGluR-dependent synaptic plasticity is blocked (Kuromi and Kidokoro 1998). Completing these experiments will provide more information about the signaling mechanism by which synaptic function is modified following acute LiGluR.activation.

Importantly, we propose to work on establishing whether presynaptic or postsynaptic function is potentiated by LiGluRs. Our mEJP recordings revealed no change in the amplitude of miniature responses after LiGluR activation. This suggests that postsynaptic LiGluR activation did not alter postsynaptic function. We also did not observe a change in the frequency of miniature response or in the paired-pulse ratio, which are two methods to assay presynaptic function. We propose a number of experiments that would determine if a presynaptic or a postsynaptic mechanism underlies the LiGluR-induced synaptic potentiation.

To determine whether postsynaptic glutamate receptors become more sensitive to glutamate, we could perform glutamate iontophoresis and test the response of postsynaptic glutamate receptors before and after acute LiGluR activation experiments (Kuromi and Kidokoro 2000; Daniels, Collins et al. 2006). If LiGluR activation does not alter responses to glutamate iontophoresis, this would indicate that the enhancement in synaptic transmission during high frequency stimulation is not due to a change in sensitivity of postsynaptic receptors to glutamate. If responses to glutamate ionotophoresis do change, this would suggest that LiGluR activation alters the sensitivity of postsynaptic glutamate receptors to evoked neurotransmission and support a postsynaptic change in synaptic strength. It is interesting to note that Concanavalin A which is used in all experiments is known to block desensitization of *Drosophila* glutamate receptors at the NMJ (Augustin, Grosjean et al. 2007). This would argue that a reduced desensitization of *Drosophila* glutamate receptors is most likely not responsible for the LiGluR-dependent synaptic strengthening during high frequency stimulation.

To investigate whether the LiGluR induced synaptic potentiation is dependent upon a releasable retrograde signal, we can perform experiments in the *syt 4* mutant background (Yoshihara, Adolfsen et al. 2005) or express tetanus toxin light chain in the muscle to inhibit postsynaptic vesicle release (Sweeney, Broadie et al. 1995). We have data showing that postsynaptic expression of tetanus toxin light chain during development reduces bouton density and evoked synaptic transmission (Figure A.3). To avoid the confounding defects of expressing postsynaptic tetanus toxin light chain, we can express it under the control of Gal80ts in only late third-instar larval muscles, possibly avoiding defects in NMJs. As an alternative explanation, LiGluRs could induce a retrograde signal that is independent of Syt 4 or postsynaptic vesicles and signal through a diffusible molecule or trans-synaptic interaction (Regehr, Carey et al. 2009).

Finally, we can repeat paired-pulse stimulation experiments before and after LiGluR activation in external solution containing low calcium. It is possible that physiological calcium (1.5 mM Ca^{++}) masks a change in PPR and doing recordings in low calcium may reveal a change in synaptic release probability. If there is a change in

PPR, it would provide evidence that acute LiGluR activation also alters synaptic release probability.

One caveat with our LiGluR activation experiments is that long-term expression of LiGluRs decreases bouton density and evoked synaptic transmission (Chapter 3). It is possible that the synaptic potentiation induced by acute LiGluR activation is dependent upon the homeostatic changes in NMJ structure and function caused by LiGluR expression. Instead these compensatory modifications could inhibit the full effect of acute postsynaptic LiGluR activation. To avoid the homeostatic effects caused by LiGluR expression during development, we expressed LiGluRs under control of Gal80ts such that we inhibited its expression early in development and only expressed LiGluRs close to third-instar larval stage. Unfortunately, we failed to fully recover LiGluR expression (Figure A.4). As an alternative, we can repeat experiments to monitor LiGluR induced synaptic potentiation with larvae expressing low affinity LiGluRs that do not exhibit homeostatic plasticity in development (Chapter 3). In addition, we can block LiGluR activity by feeding DNQX to larvae during development (Chapter 3). These experiments could verify the effect of acute LiGluR activation on synaptic function in an uncompromised background.

Figure 4.1

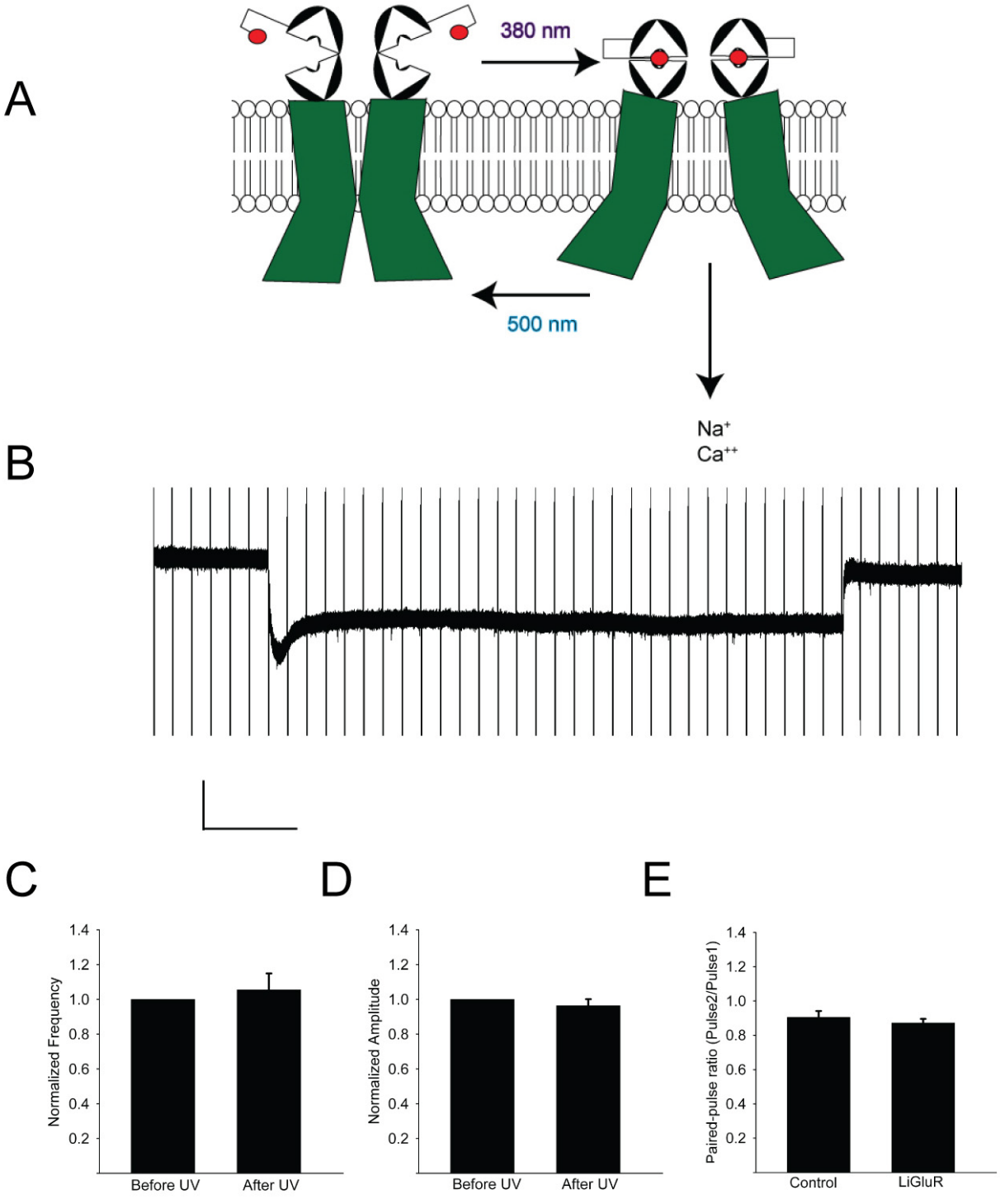
A
380 nm
500 nm
Na+
Ca++
B
C
Normalized Frequency
1.4
1.2
1.0
0.8
0.6
0.4
0.2
Before UV
After UV
D
Normalized Amplitude
1.4
1.2
1.0
0.8
0.6
0.4
0.2
Before UV
After UV
E
Paired-pulse ratio (Pulse2/Pulse1)
1.4
1.2
1.0
0.8
0.6
0.4
0.2
Control
LiGluR

Figure 4.1. Postsynaptic LiGluRs are photoswitched with 380 and 500 nm light.

Genotype used is *w*;UAS-LiGluR;24B-Gal4. **(A)** Cartoon schematic shows LiGluR activation by photoswitching of MAG that delivers glutamate to the binding pocket with 380 nm light and removes glutamate from the binding pocket with 500 nm light. **(B**) LiGluRs are activated with 10 s of 380 nm light and inactivated with 10 s of 500 nm light. LiGluR current remains active even in the absence of 380 nm light. **(C)** Averaged mEJP frequency for before and after five minute LiGluR activation. 100s of mEJP data was collected before and after LiGluR activation for each NMJ (n = 6). **(D)** Averaged mEJP amplitude for before and after LiGluR activation **(E)** Averaged paired-pulse ratio taken from 10 paired-pulses after five minute LiGluR activation. Control represents NMJs that received MAG labeling but no light (n = 4). LiGluR represents NMJs that received MAG labeling and light (n = 4). Scale is 5 nA and 50 s.

Figue 4.2

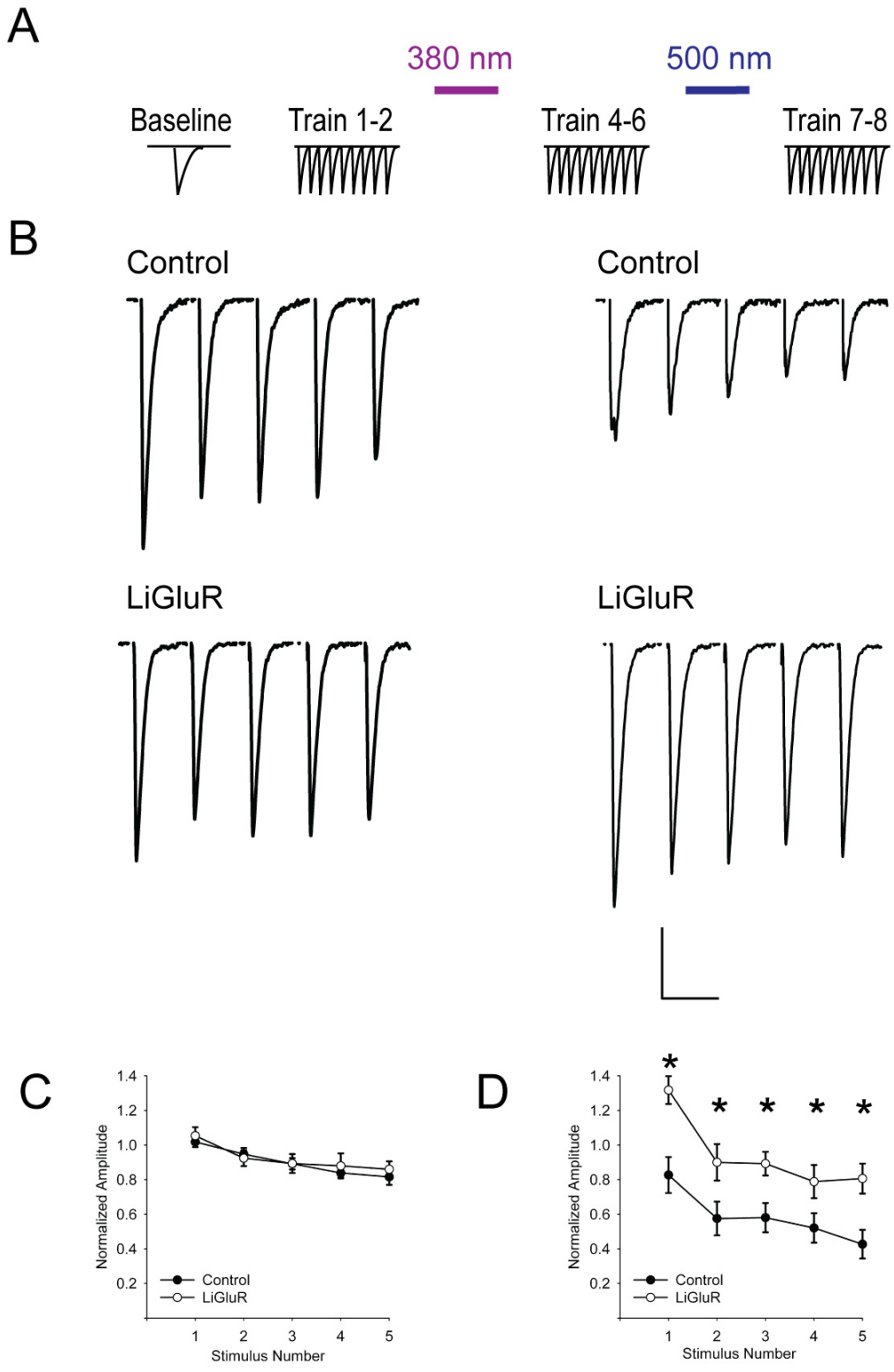
A
380 nm
500 nm
Baseline
Train 1-2
Train 4-6
Train 7-8
B
Control
Control
LiGluR
LiGluR
C
Normalized Amplitude
Control
LiGluR
Stimulus Number
D
Normalized Amplitude
Control
LiGluR
Stimulus Number

Figure 4.2. Postsynaptic LiGluR activation enhances synaptic transmission during high frequency stimulation.

Control represents NMJs that received MAG without light and LiGluR represents NMJs that received MAG and light. **(A)** Cartoon shows stimulation protocol. Initially, ten baseline evoked EJCs were recorded at 0.1 Hz. Stimulation trains were given at 20 Hz for 1 s and each train spaced 60s apart. LiGluRs were activated for 5 minutes during which trains 4-6 are recorded. **(B)** Traces show first 5 pulses of train 1 (Left) and first 5 pulses of train 8 (right) for control (n = 8) and LiGluR (n = 11) groups. **(C)** Averaged data for first 5 pulses of train 1 for control and LiGluR groups **(D)** Averaged data for first 5 pulses of train 8 for control and LiGluR groups. Scale bar is 20 nA and 50 ms

Figure 4.3

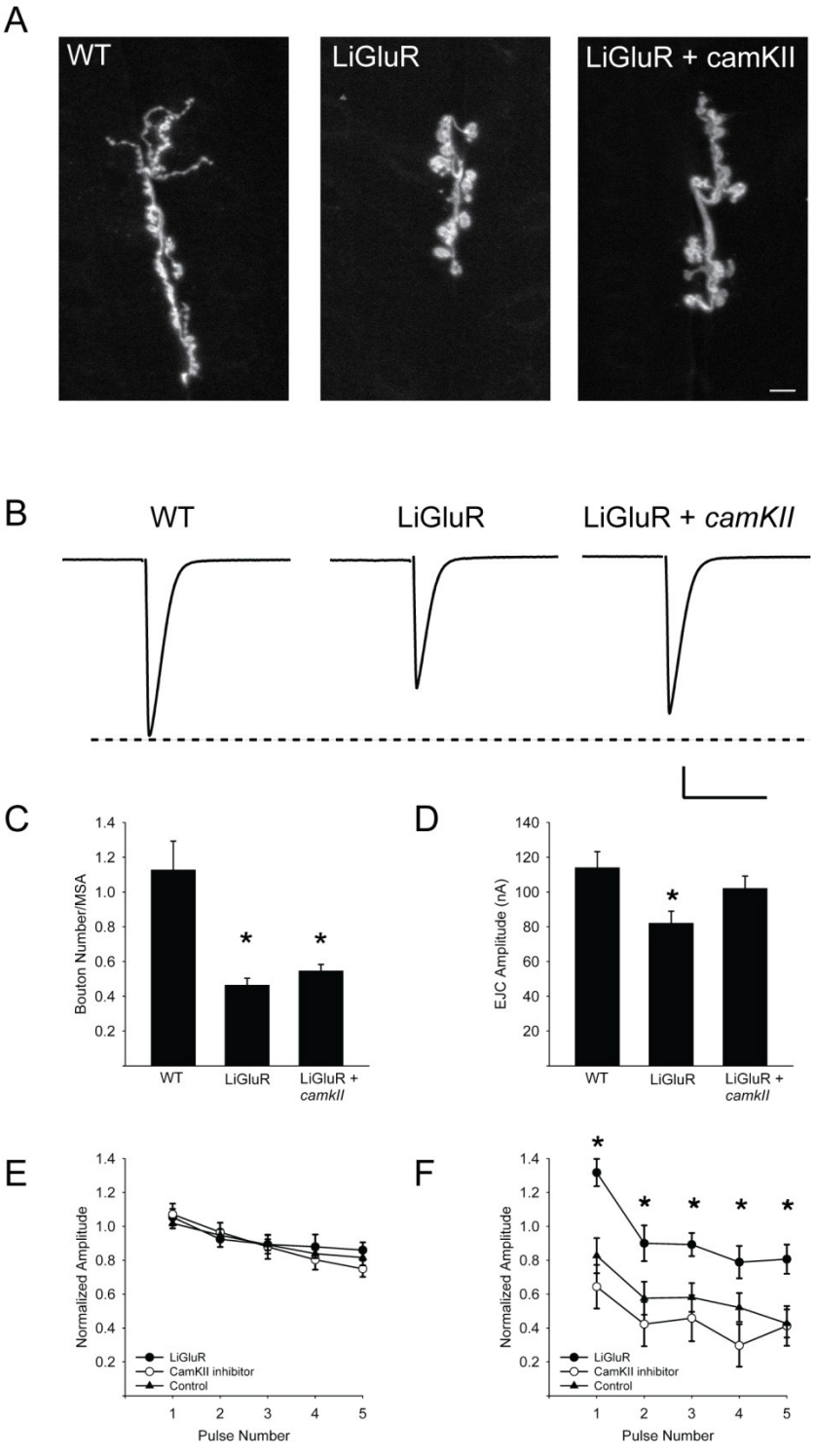
A
WT
LiGluR
LiGluR + camKII
B
WT
LiGluR
LiGluR + camKII
C
Bouton Number/MSA
WT
LiGluR
LiGluR + camkII
D
EJC Amplitude (nA)
WT
LiGluR
LiGluR + camkII
E
Normalized Amplitude
LiGluR
CamKII inhibitor
Control
Pulse Number
F
Normalized Amplitude
LiGluR
CamKII inhibitor
Control
Pulse Number

Figure 4.3. Postsynaptic CamKII activity is required for synaptic potentiation during high frequency stimulation but not for reduction in bouton density by LiGluR activity.

For all data, WT represents the genotype *w1118*;+;+, LiGluR represents *w*;UAS-LiGluR;24B, and LiGluR + *camkII* represents *w;*UAS-LiGluR,UAS-Ala/UAS-LiGluR;24B-Gal4. WT and LiGluR represent same data from Chapter 3 and shown for comparison. **(A)** Representative confocal images of HRP antibody stainings for presynaptic boutons. **(B)** Representative evoked EJC currents taken from average of 10 evoked EJCs recorded at 0.1 Hz from individual NMJ. **(C)** Averaged bouton density (bouton numbers/muscle surface area) for WT (n = 9), LiGluR (n = 8), and LiGluR + *camKII* (n = 8). **(D)** Averaged evoked EJC amplitudes for WT (n = 12), LiGluR (n = 14), and LiGluR + *camKII* (n = 12). **(E)** Averaged first five pulses for train 1 for LiGluR, control, and LiGluR + *camKII*. **(F)** Averaged first five pulses for train 8 for LiGluR, control, and LiGluR + *camKII*. LiGluR represents NMJs that received MAG and light (n = 8), control represents NMJs that received only MAG without light (n = 11), and LiGluR + *camKII* received MAG and light (n = 8). Statistical analysis performed with one-way ANOVA using Scheffe's post hoc analysis test ($p<0.05$). Scale bar for A is 10 μm. Scale bar for B is 25 nA and 20 ms.

Figure 4.4

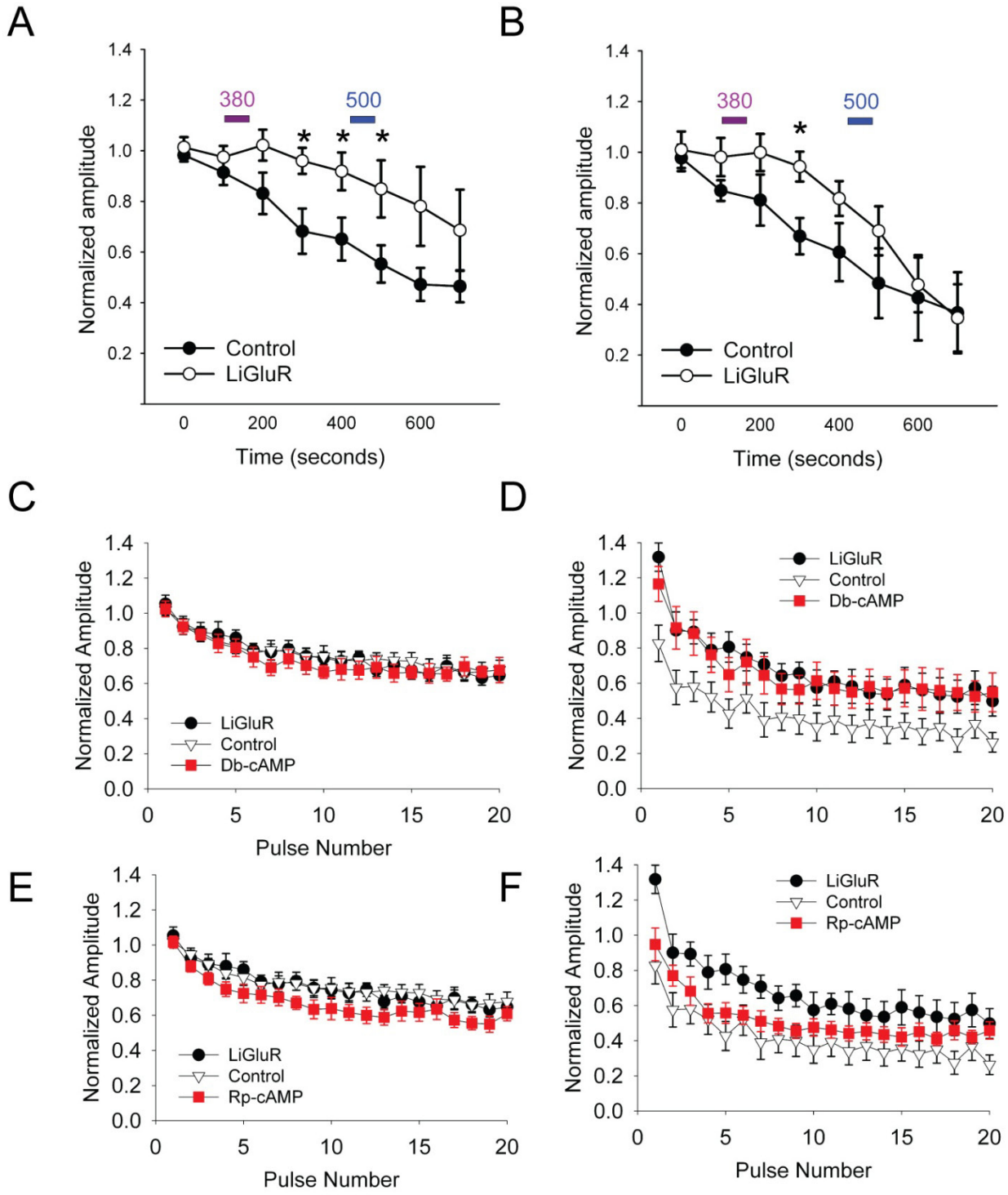
A
B
380
500
Normalized amplitude
Control
LiGluR
Time (seconds)
C
D
E
F
LiGluR
Control
Db-cAMP
Rp-cAMP
Normalized Amplitude
Pulse Number

Figure 4.4. Enhancement in synaptic transmission by LiGluR activity does not appear to require Wishful Thinking but may require cAMP signaling.

(A) Averaged first pulse of every 10 paired-pulses (50 ms interpulse interval) at 0.1 Hz for control NMJs that received MAG without light (n = 7) and LiGluR NMJs that received MAG with light (n = 7). Genotype for both groups is *w*;UAS-LiGluR;24B. **(B)** Averaged first pulse of every 10 paired-pulses (50 ms interpulse interval) at 0.1 Hz for control NMJs that received MAG without light (n = 7) and LiGluR NMJs that received MAG with light (n = 5). Genotype for both groups is *w*;UAS-LiGluR;24B,*witA12*/24B,*witB11*. **(C-D)** Averaged twenty pulses (normalized to baseline EJC amplitude) for train 1 (C) and train 8 (D) for control (NMJs that received MAG without light (n = 8)), LiGluR (NMJs that received MAG and light (n = 11)), and Db-cAMP (NMJs that received MAG and 1 mM Db-cAMP without light(n = 8)). Genotype for all groups was *w*;UAS-LiGluR;24B. **(E-F)** Averaged twenty pulses (normalized to baseline EJC amplitude) for train 1 (E) and train 8 (F) for control (NMJs that received MAG without light), LiGluR (NMJs that received MAG and light), and Rp-cAMPs (NMJs that received MAG and 100 μM Rp-cAMPs with light (n = 8)). Genotype for all groups was *w*;UAS-LiGluR;24B. Statistical analysis performed with Student's t-test ($p < 0.05$).

References

Aberle, H., A. P. Haghighi, et al. (2002). "wishful thinking encodes a BMP type II receptor that regulates synaptic growth in Drosophila." Neuron **33**(4): 545-558.

Augustin, H., Y. Grosjean, et al. (2007). "Nonvesicular release of glutamate by glial xCT transporters suppresses glutamate receptor clustering in vivo." J Neurosci **27**(1): 111-123.

Barber, C. F., R. A. Jorquera, et al. (2009). "Postsynaptic regulation of synaptic plasticity by synaptotagmin 4 requires both C2 domains." J Cell Biol **187**(2): 295-310.

Barria, A., D. Muller, et al. (1997). "Regulatory phosphorylation of AMPA-type glutamate receptors by CaM-KII during long-term potentiation." Science **276**(5321): 2042-2045.

Daniels, R. W., C. A. Collins, et al. (2006). "A single vesicular glutamate transporter is sufficient to fill a synaptic vesicle." Neuron **49**(1): 11-16.

Dobrunz, L. E. and C. F. Stevens (1997). "Heterogeneity of release probability, facilitation, and depletion at central synapses." Neuron **18**(6): 995-1008.

Frank, C. A., M. J. Kennedy, et al. (2006). "Mechanisms underlying the rapid induction and sustained expression of synaptic homeostasis." Neuron **52**(4): 663-677.

Goold, C. P. and G. W. Davis (2007). "The BMP ligand Gbb gates the expression of synaptic homeostasis independent of synaptic growth control." Neuron **56**(1): 109-123.

Gorostiza, P. and E. Y. Isacoff (2008). "Nanoengineering ion channels for optical control." Physiology (Bethesda) **23**: 238-247.

Griffith, L. C., L. M. Verselis, et al. (1993). "Inhibition of calcium/calmodulin-dependent protein kinase in Drosophila disrupts behavioral plasticity." Neuron **10**(3): 501-509.

Guerrero, G., D. F. Reiff, et al. (2005). "Heterogeneity in synaptic transmission along a Drosophila larval motor axon." Nat Neurosci **8**(9): 1188-1196.

Haghighi, A. P., B. D. McCabe, et al. (2003). "Retrograde control of synaptic transmission by postsynaptic CaMKII at the Drosophila neuromuscular junction." Neuron **39**(2): 255-267.

Hayashi, Y., S. H. Shi, et al. (2000). "Driving AMPA receptors into synapses by LTP and CaMKII: requirement for GluR1 and PDZ domain interaction." Science **287**(5461): 2262-2267.

Kazama, H., T. Morimoto-Tanifuji, et al. (2003). "Postsynaptic activation of calcium/calmodulin-dependent protein kinase II promotes coordinated pre- and postsynaptic maturation of Drosophila neuromuscular junctions." Neuroscience **117**(3): 615-625.

Kuromi, H. and Y. Kidokoro (1998). "Two distinct pools of synaptic vesicles in single presynaptic boutons in a temperature-sensitive Drosophila mutant, shibire." Neuron **20**(5): 917-925.

Kuromi, H. and Y. Kidokoro (2000). "Tetanic stimulation recruits vesicles from reserve pool via a cAMP-mediated process in Drosophila synapses." Neuron **27**(1): 133-143.

Lee, H. K., M. Barbarosie, et al. (2000). "Regulation of distinct AMPA receptor phosphorylation sites during bidirectional synaptic plasticity." Nature **405**(6789): 955-959.

Marques, G., H. Bao, et al. (2002). "The Drosophila BMP type II receptor Wishful Thinking regulates neuromuscular synapse morphology and function." Neuron **33**(4): 529-543.

Partin, K. M., D. K. Patneau, et al. (1993). "Selective modulation of desensitization at AMPA versus kainate receptors by cyclothiazide and concanavalin A." Neuron **11**(6): 1069-1082.

Poncer, J. C., J. A. Esteban, et al. (2002). "Multiple mechanisms for the potentiation of AMPA receptor-mediated transmission by alpha-Ca2+/calmodulin-dependent protein kinase II." J Neurosci **22**(11): 4406-4411.

Regehr, W. G., M. R. Carey, et al. (2009). "Activity-dependent regulation of synapses by retrograde messengers." Neuron **63**(2): 154-170.

Sweeney, S. T., K. Broadie, et al. (1995). "Targeted expression of tetanus toxin light chain in Drosophila specifically eliminates synaptic transmission and causes behavioral defects." Neuron **14**(2): 341-351.

Szobota, S., P. Gorostiza, et al. (2007). "Remote control of neuronal activity with a light-gated glutamate receptor." Neuron **54**(4): 535-545.

Volgraf, M., P. Gorostiza, et al. (2006). "Allosteric control of an ionotropic glutamate receptor with an optical switch." Nat Chem Biol **2**(1): 47-52.

Yoshihara, M., B. Adolfsen, et al. (2005). "Retrograde signaling by Syt 4 induces presynaptic release and synapse-specific growth." Science **310**(5749): 858-863.

Zucker, R. S. and W. G. Regehr (2002). "Short-term synaptic plasticity." Annu Rev Physiol **64**: 355-405.

Experimental contributions

Grant Kauwe helped with designing experiments and performed all experiments and analysis. Ehud Isacoff helped design all experiments and supervised the project.

Chapter 5

Materials and Methods

Fly Stocks

The following fly stocks were used: *w1118*, yw, UAS-Gbb-EclipticGFP, UAS-Gbb-mRFP, 24B-Gal4, Mef2-Gal4, G14-Gal4, UAS-TntxLC and UAS-IMPTNT Q4A (gifts of Kristen Scott), UAS-LiGluR, UAS-LiGluR(LA), *witA12, witB11,* and UAS-CamKII (Ala). Mutant larvae were identified with GFP or Tb marked balancers.

Gbb DNA constructs

Propeptide plus first 12 amino acids of Gbb (cDNA kindly provided by Bryan McCabe) was amplified with PCR and subcloned into the 5' end of DNA sequence encoding either mRFP or superecliptic GFP in pBluescript II KS vector. The remaining Gbb mature ligand domain was amplified with PCR and subcloned into the 3'end of these constructs. Final constructs were cut with NotI and KpnI and subcloned into pUAST vector for injection into flies.

Immunohistochemistry

Wandering third-instar larvae were dissected into a fillet on Sylgard pads in 0.45 mm Ca^{++} HL3 solution. Dissected fillets were then washed 1x with PBS. For most antibodies, fillets were fixed in 3.7% formaldehyde in PBS for 20 minutes. Some antibodies required fixation to be performed in Bouin's fixative for 5 minutes. After fixation, fillets were washed 2x with PBS and then placed in centrifuge tubes containing PBT (0.01% TritonX-100 in PBS). Fillets were then blocked with PBN (10% goat serum in PBT) for 1 hour. Primary antibody labeling was performed overnight at 4°C. Fixed samples were then washed 3x for 20 minutes in PBT. Samples were then blocked for 1 hour in PBN and then labeled with secondary antibodies for 2 h at room temperature. Fixed samples were washed 3x for 20 minutes in PBT and then placed on glass slides in 50% glycerol in PBS.

We used the following primary antibodies: anti-GFP (1:500, Invitrogen), anti-HRP (1:100, Jackson Immunoresearch), anti-GluRIIA (1:100, Developmental Hybridoma Studies Bank), and anti-GluR6 (1:500, Cell Signaling Technologies). The following secondary antibodies were used at 1:1000: Alex 647-conjugated goat anti-rabbit (Invitrogen) and Cy3-conjugated goat anti-Mouse (Jackson Immunoresearch).

Electrophysiology

Single electrode current clamp and two-electrode voltage clamp measurements were done with an Axoclamp 2B amplifier (Axon Instruments) on *Drosophila* muscle 6 at segment A3 of third instar larvae. Recording solution consisted of physiological HL3 at 1.5 mM Ca^{++} HL3 that also contained 70 mM NaCl, 5 mM KCl, 20 mM $CaCl_2$, 20 mM $MgCl_2$, 10 mM $NaHCO_3$, 5 mM Trehalose, 115 mM Sucrose, and 5 mM Hepes. In experiments with LiGluR activation, we added 2 μM Thapsigargin (Calbiochem) and 30 mg/100 mL of Concanavalin A (Sigma-Aldrich) to HL3. Recording electrodes contained 3 M KCl with resistances between 15-25 MΩ. Muscles with a membrane potential

below -60 mV and at least 4 MΩ input resistance were chosen for studies. For *wit*, LiGluR expressing larvae, we used membrane potentials of -55 mV and 2 MΩ because of the effects of the double mutant combination. Muscles were either clamped at -60 mV or -65 mV for LiGluR experiments to increase the driving force of calcium in LiGluR currents. Data was acquired at 5 KHz and were filtered at 1 KHz and recorded using a Digidata 1200A/B board and Clampex 8.0 software (Axon Instruments). Miniature synaptic transmission data was analyzed with MiniAnalysis software (Synaptosoft), and other evoked synaptic transmission data was analyzed with Clampfit 8.0 (Axon Instruments). DNQX (Tocris) was used at either 1 mM or 250 μM. Db-cAMP (Tocris) was used at 1 mM. Rp-cAMP (Tocris) was used at 100 μM. For cAMP experiments, drugs were incubated along with MAG labeling for 20 minutes before experiments and also were in recording solutions. Philanthotoxin-433 was purchased from Sigma-Aldrich.

MAG labeling

Third-instar larvae were dissected into a fillet in 0.45 mM Ca^{++} HL3 solution. Fillets were then incubated with the brain intact for 12 minutes in 1.5 mM Ca^{++} HL3 with 2 μM Thapsigargin and 30 mg/100 mL of Concanavalin A. HL3 solution was removed and replaced with 50 μM of MAG-0 (kindly provided by Dirk Trauner) in 0.45 mM Ca^{++} HL3 which had been preilluminated with 380 nm light for 3 minutes (1% final DMSO concentration). Fillets were incubated in MAG for 20 minutes in dark. MAG was removed and fillets were washed 2x with 1.5 mM Ca^{++} HL3. Preparations were illuminated with Lambda LS 300W Xenon arc lamp system (Sutter) with excitation filters of 380/30 nm and HQ470/40 (Chroma).

Appendix

Additional experiments

Figure A.1

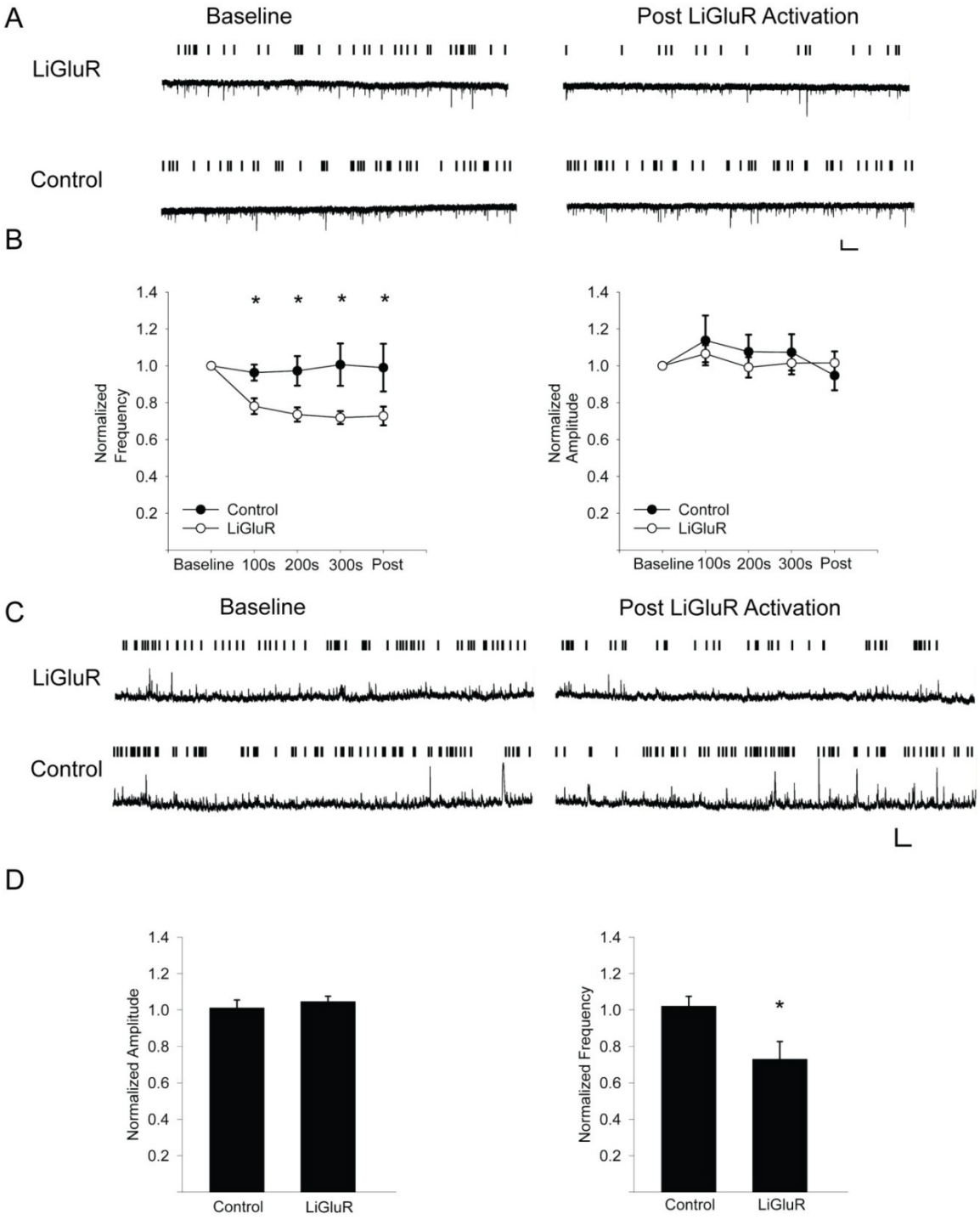
A
Baseline
Post LiGluR Activation
LiGluR
Control
B
Normalized Frequency
Normalized Amplitude
Control
LiGluR
Baseline 100s 200s 300s Post
C
Baseline
Post LiGluR Activation
LiGluR
Control
D
Normalized Amplitude
Normalized Frequency
Control
LiGluR

Figure A.1. Rapid postsynaptic LiGluR activation leads to a decrease in spontaneous miniature frequency without a change in amplitude SynapCaM background.

All data is represented by the genotype SynapCaM;UAS-LiGluR;24B-Gal4. **(A)** Representative mEJC traces show baseline data taken from before LiGluR activation (left) and mEJC traces from the same NMJs after LiGluR activation (right). LiGluR represents NMJs that received MAG and light, and control represents NMJs that received only MAG without light. **(B)** Averaged mEJC frequency (left) and amplitude (right) normalized to baseline values. Each time point represents the average of 100s of data. Data shows a significant decrease in mEJC frequency in LiGluR activation group (n = 16) compared to control (n = 12) **(C)** Representative mEJP traces show baseline data taken from before LiGluR activation (left) and mEJP traces from the same NMJs after LiGluR activation (right). **(D)** Averaged mEJP amplitude (left) and frequency (right) normalized to baseline values. Data shows a significant decrease in mEJP frequency in LiGluR activation group (n = 6) compared to control (n = 6). Statistical analysis performed with Student's t-test ($p < 0.05$). Scale is 0.5 nA and 1s for A. Scale is 1 mV and 2s for C.

Figure A.2

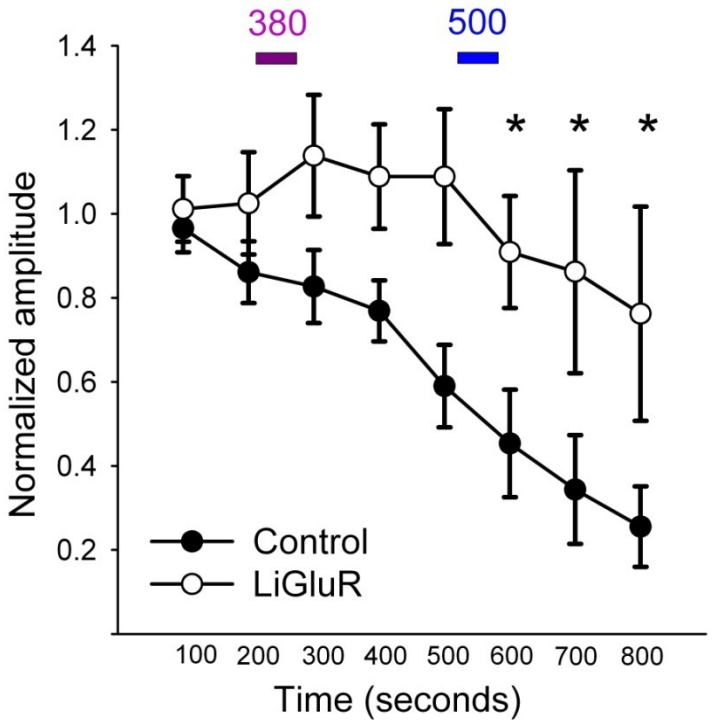

Figure A.2. Synaptic potentiation induced by postsynaptic LiGluR activation is not blocked in the *wishful thinking* mutant.

Genotype represented is *w*;UAS-LiGluR;24B,*witA12*/24B, *witB11*. Averaged first pulse normalized amplitude data shown from paired-pulse (50 ms IPI 1st two time points and 30 ms IPI for remaining time points) recordings. Control represents NMJs that received MAG without light and LiGluR represents NMJs that received MAG and light. Acute postsynaptic LiGluR activation significantly induces synaptic potentiation in the *wit* mutant. Statistical analysis performed with two-tailed Student's t-test ($p < 0.05$).

Figure A.3

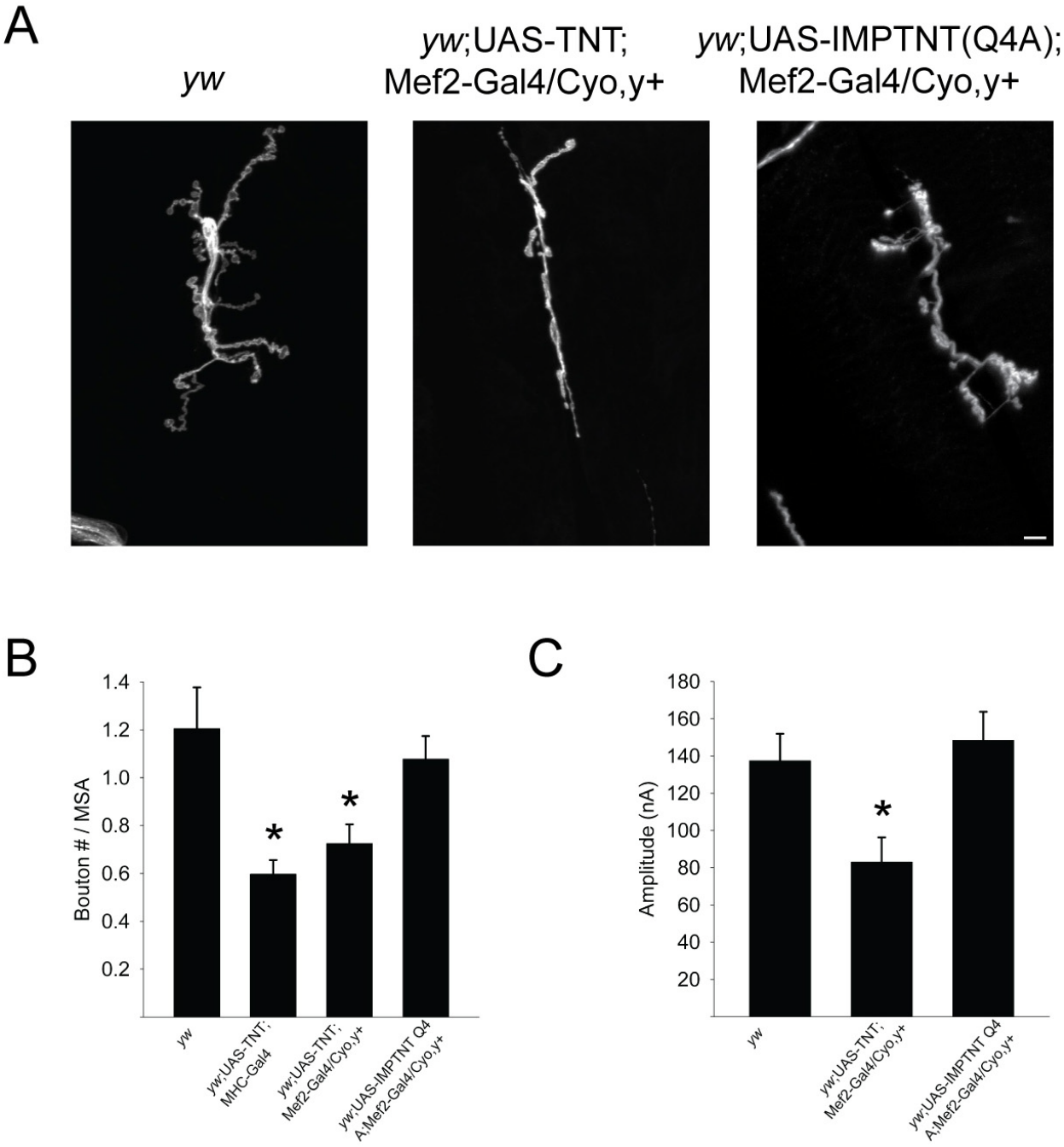
A
yw
yw;UAS-TNT;
Mef2-Gal4/Cyo,y+
yw;UAS-IMPTNT(Q4A);
Mef2-Gal4/Cyo,y+
B
Bouton # / MSA
1.4
1.2
1.0
0.8
0.6
0.4
0.2
*
*
yw
yw;UAS-TNT;
MHC-Gal4
yw;UAS-TNT;
Mef2-Gal4/Cyo,y+
yw;UAS-IMPTNT Q4
A,Mef2-Gal4/Cyo,y+
C
Amplitude (nA)
180
160
140
120
100
80
60
40
20
*
yw
yw;UAS-TNT;
Mef2-Gal4/Cyo,y+
yw;UAS-IMPTNT Q4
A,Mef2-Gal4/Cyo,y+

Figure A.3. Postsynaptic expression of tetanus toxin light chain reduces bouton density and evoked EJC amplitude.

(A) Representative confocal images of HRP antibody staining for presynaptic boutons. **(B)** Averaged bouton density (bouton number / muscle surface area) for *yw* (n = 7), tetanus toxin expressed with MHC-Gal4 (n = 9), tetanus toxin expressed with Mef2-Gal4 (n = 8), and inactive tetanus toxin expressed with Mef2-Gal4 (n = 12). Postsynaptic expression of tetanus toxin with either muscle expressing Gal4 drivers, MHC-Gal4 or Mef2-Gal4, result in a significant decrease in bouton density. **(C)** Averaged evoked EJC amplitudes for *yw* (n = 10), tetanus toxin expressed with Mef2-Gal4(n = 13), and inactive tetanus toxin expressed with Mef2-Gal4 (n = 9). Postsynaptic expression of tetanus toxin with Mef2-Gal4 results in a significant decrease in evoked EJC amplitude. Statistical analysis performed with one-way ANOVA and Scheffe's post hoc analysis test ($p < 0.05$). Scale bar is 10 μm.

Figure A.4

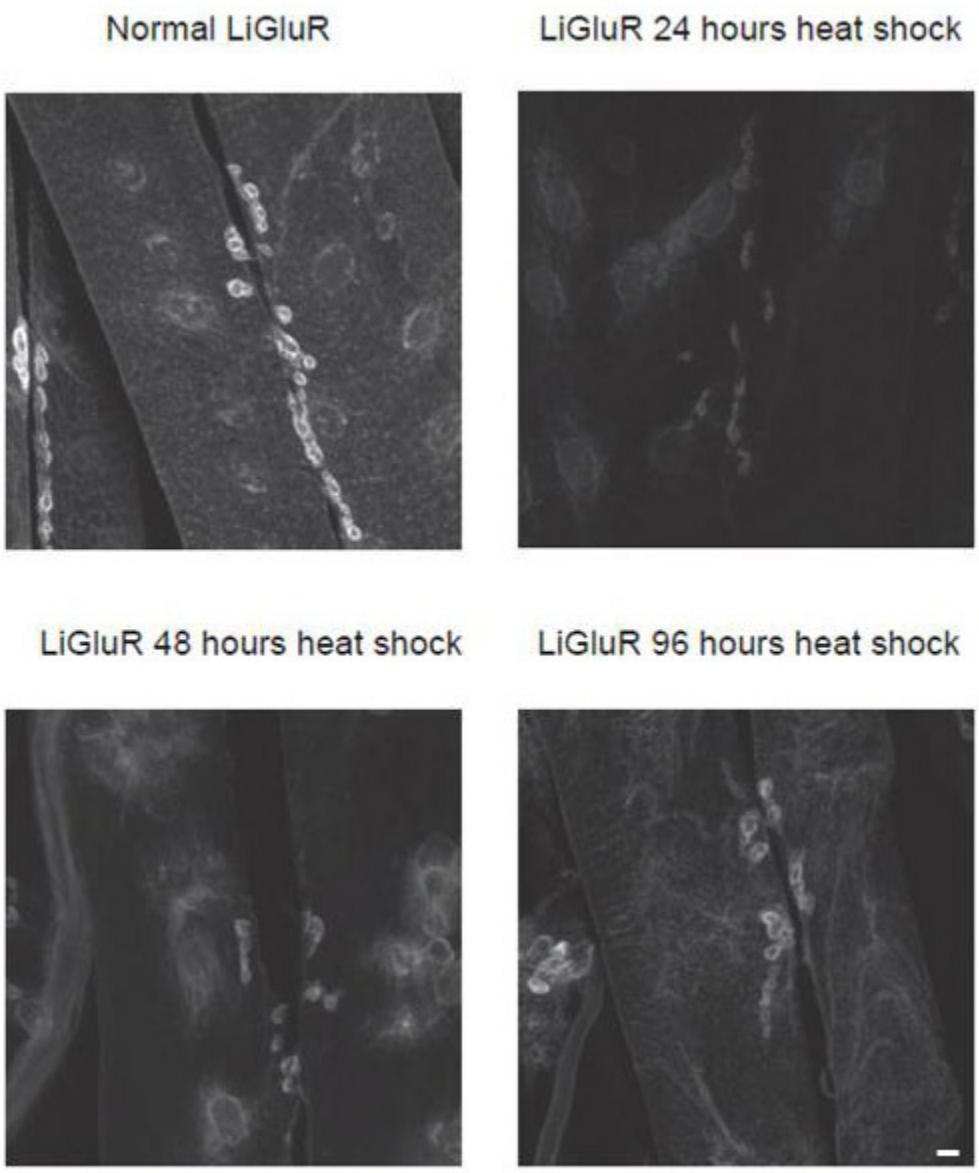
Normal LiGluR
LiGluR 24 hours heat shock
LiGluR 48 hours heat shock
LiGluR 96 hours heat shock

Figure A.4. Gal80ts control of LiGluRs results in weak expression.

Genotype for conditional expression of LiGluRs is *w*;UAS-LiGluR;24B-Gal4,tub-Gal80ts. Larvae were raised at 18°C (restrictive temperature) and heat shocked larvae at 30°C (permissive temperature) for different times. Representative confocal images show antibody stainings to GluR6 (LiGluRs). All preparations were stained under the same treatment. Normal LiGluR (top left) shows an image of antibody staining to NMJ expressing LiGluR only under Gal4 control (*w*;UAS-LiGluR;24B). Remaining three panels show images from antibody stainings of larvae that were heat shocked for their respective times. Our longest heat shock of 96 hours fails to restore LiGluR expression to levels similar to that of NMJs that express LiGluRs continuously throughout development. Scale bar is 10 μm.

Figure A.5

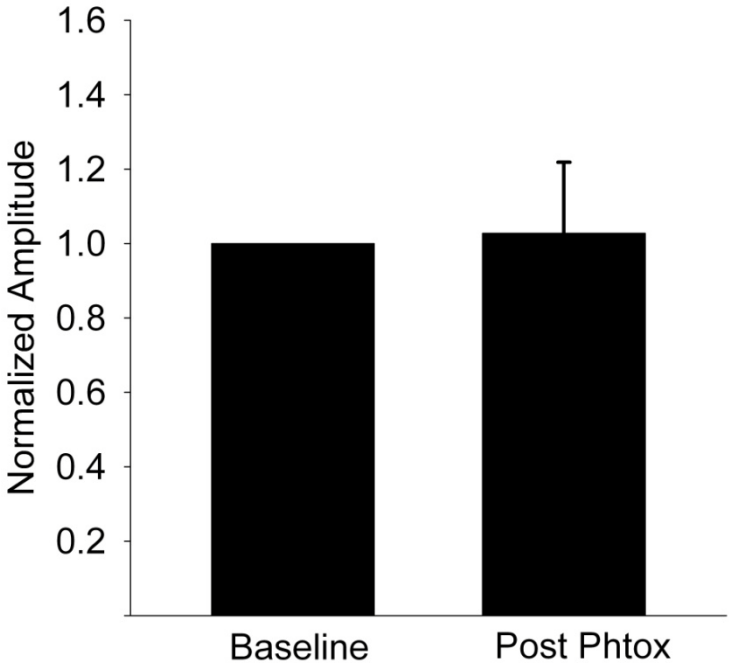

Figure A.5. Philanthotoxin fails to reduce evoked EJP amplitude.

Experiments were performed according to published literature (Frank, Kennedy et al. 2006; Goold and Davis 2007). Briefly, experiments were done in 0.6 mM Ca^{++} in third-instar larvae at muscle 6. Ten baseline evoked EJPs were recorded at 0.1 Hz after which philanthotoxin was applied to bath solution for a final concentration of 4 μM. Recordings resumed and ten evoked EJPs were then collected. For each NMJ, the average of ten evoked EJPs was calculated and data was normalized to baseline values. We did not observe a decrease in evoked EJPs as a result of philanthotoxin application (n = 9). Previous experiments showed that evoked EJP amplitude decreases in seconds upon philanthotoxin bath application (Frank, Kennedy et al. 2006).

Figure A.6

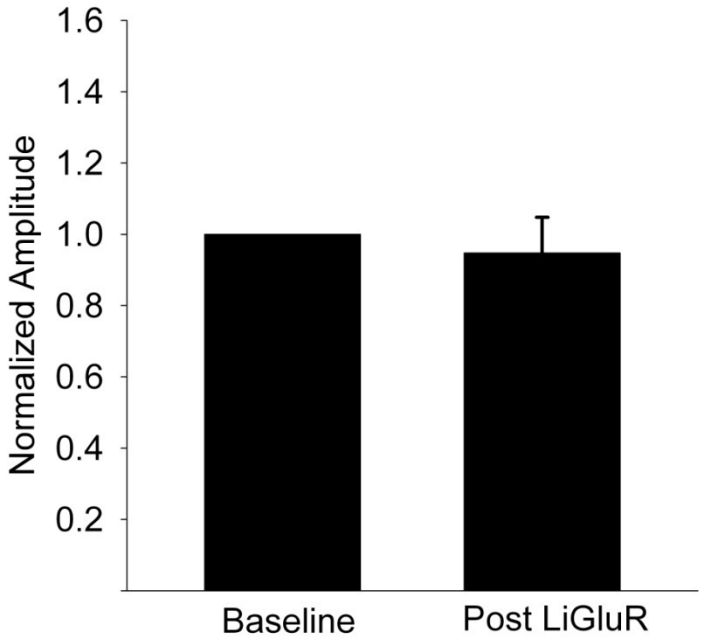

Figure A.6. Single evoked EJCs do not change in amplitude with LiGluR activation.

Genotype represented by data is SynapCaM;UAS-LiGluR;24B-Gal4. We stimulated NMJs with single pulses at 0.1 Hz and averaged every 10 evoked EJCs. Data was normalized to baseline values collected before five minute LiGluR activation. We show that averaged evoked EJC amplitudes collected after LiGluR activation do not change from baseline values (n = 7).